Accepted Manuscript

Discovery of novel hybrids of diaryl-1,2,4-triazoles and caffeic acid as dual inhibitors of cyclooxygenase-2 and 5-lipoxygenase for cancer therapy

Hao Cai, Xiaojing Huang, Shengtao Xu, Hao Shen, Pengfei Zhang, Yue Huang, Jieyun Jiang, Yijun Sun, Bo Jiang, Xiaoming Wu, Hequan Yao, Jingyi Xu

PII: S0223-5234(15)30350-0

DOI: 10.1016/j.ejmech.2015.11.013

Reference: EJMECH 8203

To appear in: *European Journal of Medicinal Chemistry*

Received Date: 11 August 2015

Revised Date: 16 October 2015

Accepted Date: 6 November 2015

Please cite this article as: H. Cai, X. Huang, S. Xu, H. Shen, P. Zhang, Y. Huang, J. Jiang, Y. Sun, B. Jiang X. Wu, H. Yao, J. Xu, Discovery of novel hybrids of diaryl-1,2,4-triazoles and caffeic acid as dual inhibitors of cyclooxygenase-2 and 5-lipoxygenase for cancer therapy, *European Journal of Medicinal Chemistry* (2015), doi: 10.1016/j.ejmech.2015.11.013.

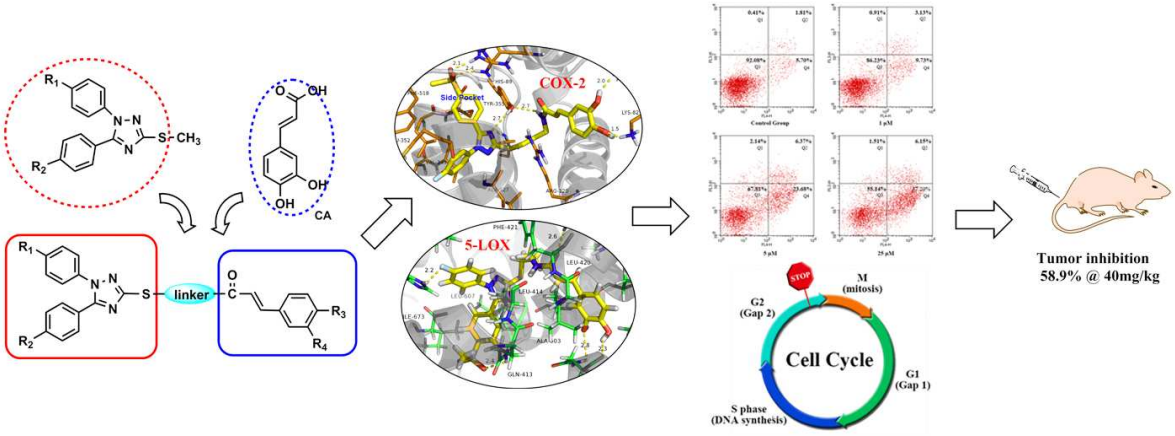

Discovery of novel hybrids of diaryl-1,2,4-triazoles and caffeic acid as dual inhibitors of cyclooxygenase-2 and 5-lipoxygenase for cancer therapy

Hao Cai[a,b], Xiaojing Huang[a,b], Shengtao Xu[a,b], Hao Shen[a,b], Pengfei Zhang[a,b], Yue Huang[a,b], Jieyun Jiang[c], Yijun Sun[d], Bo Jiang [a,b], Xiaoming Wu[a,b,*], Hequan Yao[a,b], Jingyi Xu[a,b,*]

[a] *Department of Medicinal Chemistry, China Pharmaceutical University, 24 Tong Jia Xiang, Nanjing 210009, China*

[b] *State Key Laboratory of Natural Medicines, China Pharmaceutical University, Nanjing 210009, P. R. China.*

[c] *Department of Microbiology, Immunology and Molecular Genetics, University of Kentucky College of Medicine, Lexington, KY 40536, USA*

[d] *Drug Screening Center, Nanjing KeyGen Biotech. Co. Ltd., Nanjing 210012, China*

* Corresponding authors. Department of Medicinal Chemistry, China Pharmaceutical University, 24 Tong Jia Xiang, Nanjing 210009, P R China.

E-Mail addresses: xmwu@cpu.edu.cn (X. Wu), jinyixu@china.com (J. Xu).

Abstract: Inflammation plays a key role in cancer initiation and propagation. Cyclooxygenase-2 (COX-2) and 5-lipoxygenase (5-LOX), two important enzymes in inflammatory responses are up-regulated in various tumor types. Dual inhibition of COX-2 and 5-LOX constitutes a rational concept for the design of more efficacious anti-tumor agents with an improved safety profile. We have previously reported a series of diaryl-1,2,4-triazole derivatives as selective COX-2 inhibitors. Herein, we hybridized the diaryl-1,2,4-triazoles with caffeic acid (CA) which was reported to display 5-LOX inhibitory and anti-tumor activities, affording a novel class of COX-2/5-LOX dual inhibitors as anti-tumor drug candidates. Most of these compounds exhibited potent COX-2/5-LOX inhibitory and antiproliferative activities *in vitro.* And the most potent compound **22b** could significantly inhibit tumor growth *in vivo*. Furthermore, mechanistic investigation showed that the representative compound **15c** blocked cell cycle in G2 phase and induced apoptosis in human non-small cell lung cancer A549 cells in a dose-dependent manner. Our preliminary investigation results would provide new clues for the cancer theatment with COX-2/5-LOX dual inhibitors.

Keywords: Cyclooxygenase-2; 5-Lipoxygenase; Diaryl-1,2,4-Triazoles; Caffeic acid; Anti-tumor activity.

1. Introduction

Inflammation is a complex process that involves widespread changes in cellar and molecular components of physiology. Controlled inflammation is necessary for a series of protective process including wound healing, tissue repair and defense against pathogens. However, prolonged chronic inflammation is mostly detrimental and has been linked to a number of diseases, including cancer [1-3]. Recent studies have validated the postulation that within the tumor microenvironment, a network of various pro-inflammatory mediators participate in complex signaling process that facilitates extravasations of tumor cells through the stroma promoting the development of carcinogenesis [4].

Rarchidonic acid (AA), an essential polyunsaturated fatty acid with 20 carbons is the major precursor of several classes of signal molecules which are important mediators in inflammatory responses. The two main metabolic pathways of AA are cyclooxygenase (COX) and lipoxygenase (LOX) pathways. AA is converted to prostaglandins, prostacyclins and thromboxanes by COX and to hydroxyeicosatetraenioc acids (HETEs) or leukotrienes (LTs) by LOX. Recent studies regarding the relationship between AA metabolic process and carcinogenesis reveal novel molecular target for cancer treatment [5].

It has been reported that COX-2 is up-regulated in various tumor types, such as pancreatic, prostate and colorectal cancers [6-8], resulting in elevation of downstream prostaglandin E_2 (PGE_2) levels [9]. Lots of results indicate that PGE_2 could increase the motility and metastic potential of tumor cells, promote tumor angiogenesis, induce local immunosuppression and inhibit apoptosis [5, 10]. Besides PGE_2 mechanism, COX-2 itself could also conduces to carcinogens. COX-2 peroxidase activity is able to transform many procarciogens into ultimate carcinogens which can active many genes involved in cell proliferation [5, 11]. Furthermore, COX-2 could also promote cancer cell survival through lowering the levels of unesterified AA [12]. Inhibition of COX-2 activity has been shown to induce apoptosis and inhibit proliferation and angiogenesis [13, 14].

Similar to COX-2, the expression and activity of 5-LOX have been found to be up-regulated in many cancer cell lines [15-19], and closely related to tumor size, depth and vessel invasion [20]. It is evident from recent studies that 5-LOX and its downstream products leukotriene B_4 (LTB_4) and 5-hydroxyeicosatetranoic acid (5-HETE) could enhance cell proliferation and suppress apoptosis, thereby promoting the development of carcinogenesis [15, 18, 19, 21-24]. It seems likely that COX-2 and 5-LOX may represent an integrated system that regulates the proliferation, metastatic and proangiogenic potential of cancer cells [5]. Considering the frequent co-expression of these two enzymes and the striking analogy of their biological functions, dual inhibitors of COX-2 and 5-LOX may present a superior anticancer profile in carcinogenesis. And notably, there is a cross-talk between COX-2 and 5-LOX pathways, inhibition of only one of them would shunt AA metabolism to the other pathway, thereby inducing potential side effects [25]. Hence the dual COX-2/5-LOX inhibitors would also be safer. Overall, dual inhibition of COX-2 and 5-LOX constitutes a rational concept for the design of more efficacious anti-tumor agents with an improved safety profile.

Triazole heterocycle is a building block of great value in drug candidates[26, 27]. Recently, we have identified a series of 1,5-diaryl-1,2,4-trizole derivatives as selective COX-2 inhibitors, among which compound **1** (Fig. 1) displayed potent and selective COX-2 inhibitory activity (IC_{50} = 0.37 μM, SI = 0.018), equipotent to that of celecoxib (IC_{50} = 0.26 μM, SI = 0.015) [28].

Successively, we developed a series of diaryl-1,2,4-triazoles bearing N-hydroxyurea moiety as COX-2/5-LOX dual inhibitors for anti-inflammation [29]. Inspired by the obtained interesting results of our previous studies and in continuation of our endeavor for novel anticancer drugs, we became interest in exploring dual COX-2/5-LOX inhibitors as anti-tumor candidates with novel structural characteristics, better anticancer effects and improved safety profiles. Meanwhile, we noticed that the caffeic acid (CA), a widespread phenolic compound from the group of hydroxycinnamates, selectively inhibits 5-LOX [30] and a novel series of triazole-containing caffeic acid analogues was reported as 5-LOX inhibitors recently[31]. Moreover, CA and its derivatives, for instance, phenethyl caffeate (CAPE) could also inhibit the growth and differentiation of various cancer cells, promote apoptosis and prevent chemical carcinogenesis [32-35]. However, it has been found that CA has a stimulatory effect on prostaglandin synthase, which may result from its stimulation on COX pathway [30]. Accordingly, we hybridized the CA scaffold with the selective COX-2 inhibitory moiety of compound **1** (Fig. 2) and designed a series of 1,5-diarylsubstituted-1,2,4-triazole derivatives as COX-2/5-LOX dual inhibitors for anticancer candidates. Herein we report the synthesis, *in vitro* and *in vivo* biological evaluation and docking studies of these novel hybrids.

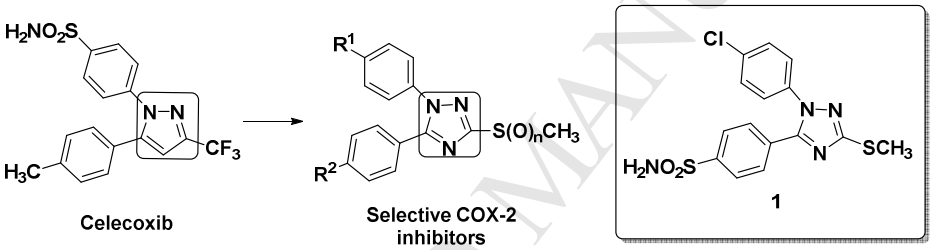

Fig. 1. 1,5-diaryl-1,2,4-triazole derivatives as selective COX-2 inhibitors.

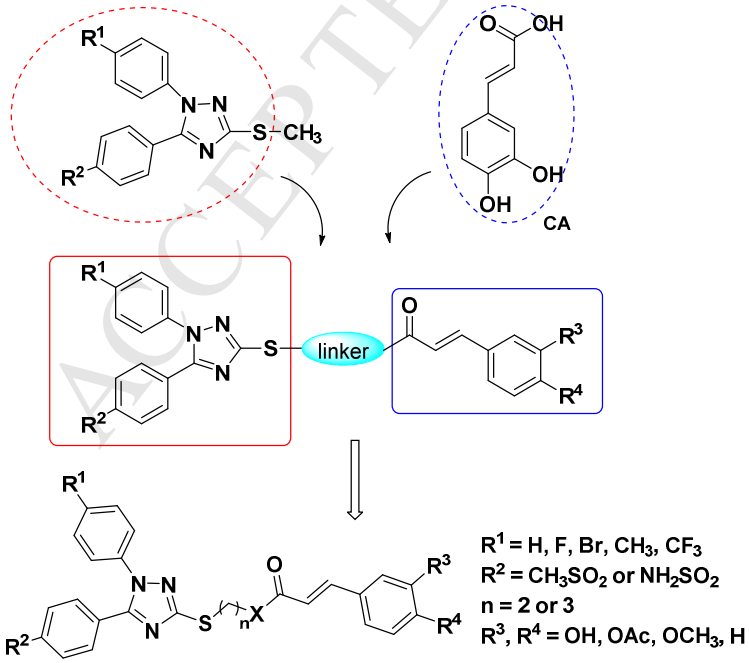

Fig. 2. Hybrids of CA and diaryl-1.2.4-triazoles as dual COX-2/5-LOX dual inhibitors.

2. Results and discussion

2.1 Chemistry

The 1,5-diphenyl-1,2,4-triazole-3-thiol (**6a-i**) were prepared from corresponding phenyl hydrazine and benzoyl chloride as described in our previous report [28] (Scheme 1). Subsequent treatment of the intermediate **6a-g** with ethyl bromoacetate or ethyl 3-bromopropionate in the presence of K_2CO_3, followed by reduction using $LiAlH_4$, afforded the respective 1,5-diphenyl-1,2,4-triazol-3-thioalkylol (**8a-f**). Then the hydroxyl group of 8**a-e** was transformed into triazo group. And the triazo group could be reduced to amino group through Staudinger reaction, yielding the intermediates **11a-e** (Scheme 2).

The synthesis of CA esters is outlined in Scheme 3. Acetylation of hydroxyl groups of CA provided corresponding ester **12**, which was subsequently reacted with 1,2-dibromoethane or 1,3-dibromopropane, respectively, in presence of Et_3N in acetone, to produce intermediates **13a-b**. Condensation of **13a-b** with 1,2,4-triazole-3-thiol **6a-b**, **6d-e**, **6g-i** in the presence of K_2CO_3 afforded compounds **14a-n**. Deprotection of **14b**,**d**,**e**,**k**,**o** using 30% MeONa in MeOH yielded target compounds **15a-e**. The target compounds bearing *p*-NH_2SO_2 moiety at C-5 phenyl ring were obtained by deprotection of *tert*-butyl in CF_3COOH–$PhOCH_3$ solution.

And the synthesis route of CA amide derivatives is shown in Scheme 4.Protection of the hydroxyl groups of CA as an acetate followed by reaction with thionyl chloride afforded the acyl chloride **13**. Condensation of **13** with 1,2,4-triazole-3-thioalkylamine (**11a-e**) in the presence of TEA given corresponding amides **17a-g**. Subsequently, **17c** was deprotected in condition of MeONa providing the target product **18**.

Besides, we substituted the *meta*-hydroxyl group of CA phenyl ring with methoxyl group and obtained a series of ferulaic acid esters. Different from CA, the ferulaic acid was protected with Ac_2O in the presence of concentrated H_2SO_4 (Scheme 5) and the other operation steps were similar to those in Scheme 3.

At last, both of the hydroxyl groups of CA were removed resulting in cinnamic acid ester derivatives. These compounds (**23a, b**) could be directly prepared by treating 1,2,4-triazol-3-thioalkylol (**8d** of **8f**) with cinnamic acid in the presence of DCC and DMAP in dichloromethane (Scheme 6). And deprotection of **23b** afforded the target compound **23c** (Scheme 6)**.**

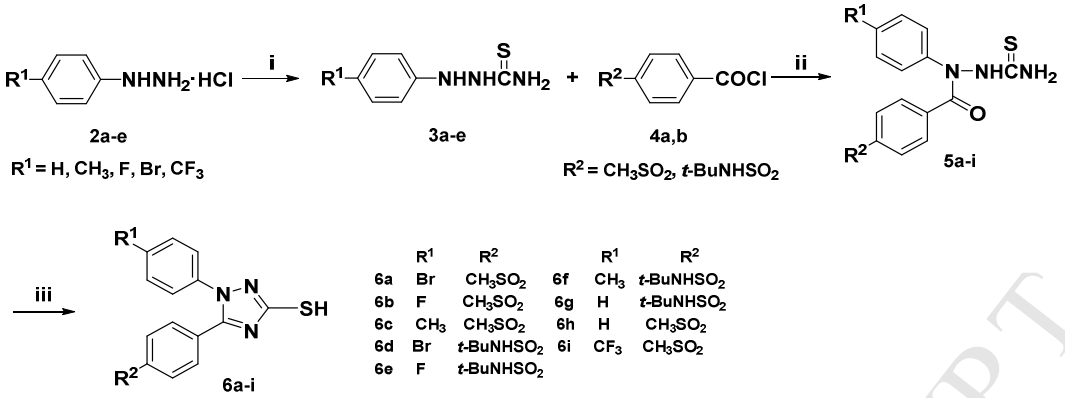

	R1	R2		R1	R2
6a	Br	CH_3SO_2	6f	CH_3	*t*-BuNHSO$_2$
6b	F	CH_3SO_2	6g	H	*t*-BuNHSO$_2$
6c	CH_3	CH_3SO_2	6h	H	CH_3SO_2
6d	Br	*t*-BuNHSO$_2$	6i	CF_3	CH_3SO_2
6e	F	*t*-BuNHSO$_2$			

Scheme 1. Synthesis of 1,5-diphenyl-1*H*-1,2,4-triazole-3-thiol (**6a-i**). *Reagent and conditions*: (i) KSCN, conc. HCl, anhydrous alcohol, reflux, 5 h; (ii) Et_3N, acetone, reflux, 2 h; (iii) a.10% NaOH, MeOH, reflux, 2 h; b.10% HCl.

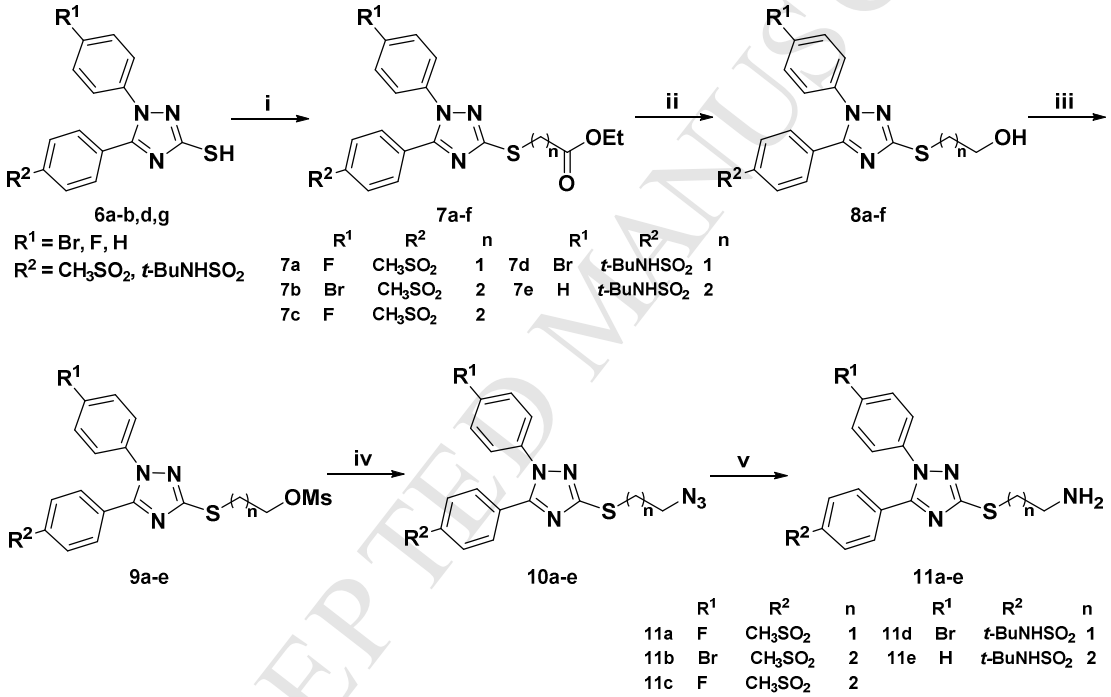

	R1	R2	n		R1	R2	n
7a	F	CH_3SO_2	1	7d	Br	*t*-BuNHSO$_2$	1
7b	Br	CH_3SO_2	2	7e	H	*t*-BuNHSO$_2$	2
7c	F	CH_3SO_2	2				

	R1	R2	n		R1	R2	n
11a	F	CH_3SO_2	1	11d	Br	*t*-BuNHSO$_2$	1
11b	Br	CH_3SO_2	2	11e	H	*t*-BuNHSO$_2$	2
11c	F	CH_3SO_2	2				

Scheme 2. Synthesis of Synthesis of 1,5-diphenyl-1*H*-1,2,4-triazole-3-thioalkylamine (**11a-e**). *Reagents and conditions*: (i) ethyl bromoacetate or ethyl 3-bromopropionate, K_2CO_3, acetone, reflux, 3 h; (ii) LAH, dry THF, reflux, 3 h; (iii) MsCl, DCM, 0 ^oC, 2 h; (iv) sodium azide, DMF, 80 ^oC, 3 h; (v) triphenylphosphine, H_2O, THF, r.t., 6 h.

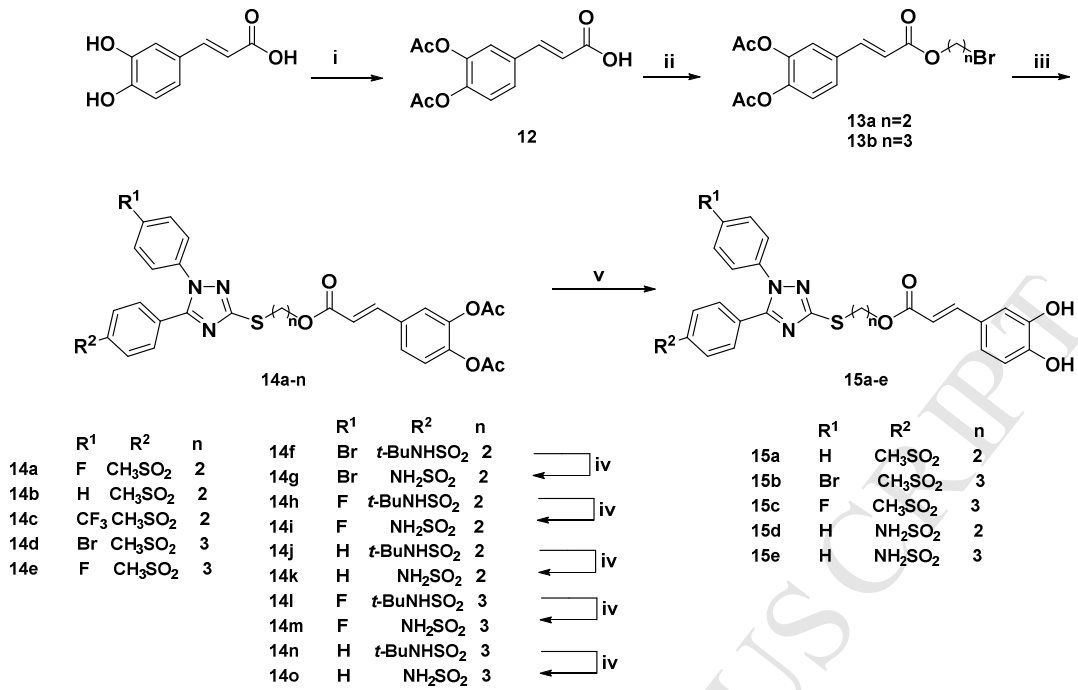

	R^1	R^2	n
14a	F	CH_3SO_2	2
14b	H	CH_3SO_2	2
14c	CF_3	CH_3SO_2	2
14d	Br	CH_3SO_2	3
14e	F	CH_3SO_2	3

	R^1	R^2	n
14f	Br	*t*-BuNHSO$_2$	2
14g	Br	NH_2SO_2	2
14h	F	*t*-BuNHSO$_2$	2
14i	F	NH_2SO_2	2
14j	H	*t*-BuNHSO$_2$	2
14k	H	NH_2SO_2	2
14l	F	*t*-BuNHSO$_2$	3
14m	F	NH_2SO_2	3
14n	H	*t*-BuNHSO$_2$	3
14o	H	NH_2SO_2	3

	R^1	R^2	n
15a	H	CH_3SO_2	2
15b	Br	CH_3SO_2	3
15c	F	CH_3SO_2	3
15d	H	NH_2SO_2	2
15e	H	NH_2SO_2	3

Scheme 3. Synthesis of affeic acid esters. *Reagent and conditions*: (i) a. DMAP, DCM, reflux, 5 min; b. acetic anhydride, TEA, reflux 4 h; (ii) 1,2-dibromoethane or 1,3-dibromopropane, TEA, acetone, reflux, 24 h; (iii) **6a-b**, **6d-e**, **6g-i**, K_2CO_3, acetone, r.t., 5-10 h; (iv) TFA/methylanisole, 0 ^{o}C-r.t., 24 h; (v)MeONa/MeOH (30 %), 0 ^{o}C-r.t., 15-30 min.

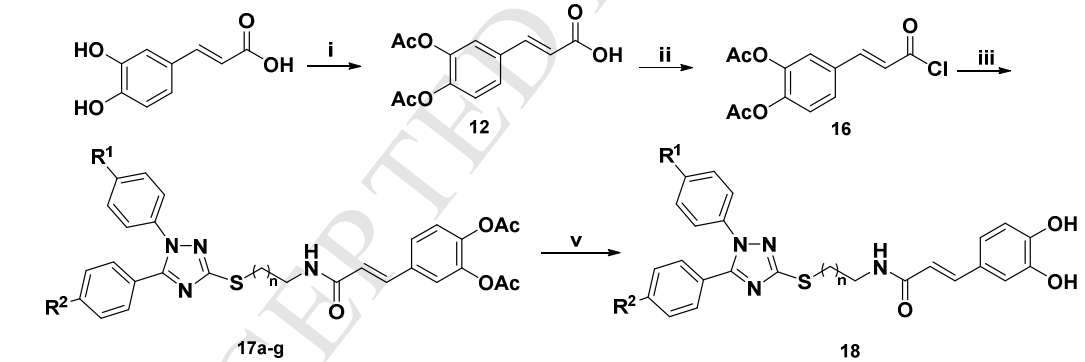

	R^1	R^2	n
17a	F	CH_3SO_2	1
17b	Br	CH_3SO_2	2
17c	F	CH_3SO_2	2

	R^1	R^2	n
17d	Br	*t*-BuNHSO$_2$	1
17e	Br	NH_2SO_2	1
17f	H	*t*-BuNHSO$_2$	2
17g	H	NH_2SO_2	2

	R^1	R^2	n
18	F	CH_3SO_2	2

Scheme 4. Synthesis of CA amides. *Reagent and conditions*: (i) a. DMAP, DCM, reflux, 5 min; b. acetic anhydride, TEA, reflux 4 h; (ii) thionyl chloride, reflux, 3 h; (iii) **11a-e** TEA, DCM, 0^{o}C-r.t., 8 h; (iv) TFA/methylanisole, 0 ^{o}C-r.t., 24 h; (v) MeONa/MeOH (30 %), 0 ^{o}C-r.t., 15-30 min.

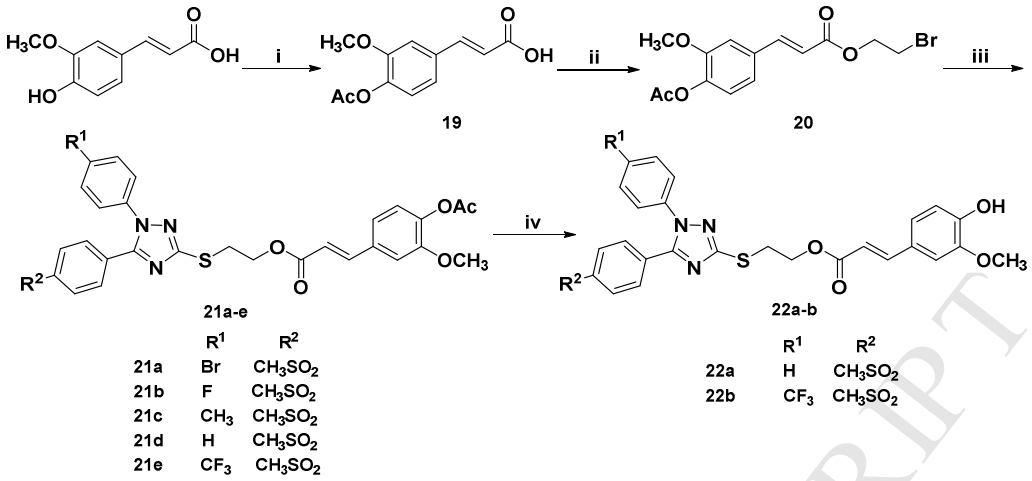

Scheme 5. Synthesis of ferulaic acid esters. *Reagent and conditions*: (i) Ac_2O, conc. H_2SO_4, r.t., 10-15 min; (ii) 1,2-dibromoethane, TEA, acetone, reflux, 24 h; (iii) **6a-c** or 6**h-i,** K_2CO_3, acetone, r.t., 5-10 h; (iv) MeONa/MeOH (30 %), 0 ^oC-r.t., 15-30 min.

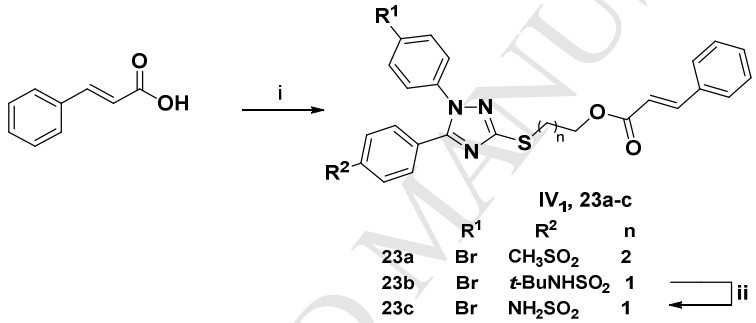

Scheme 6. Synthesis of cinnamic acid esters. *Reagent and conditions*: (i) **8b** or **8f**, DCC, DMAP, DCM, r.t., overnight; (ii) TFA/methylanisole, 0 ^oC-r.t., 24 h.

2.2 *In Vitro* COX-2 and 5-LOX inhibitory activities

The obtained hybrids of CA and diaryl-1.2.4-triazoles were evaluated *in vitro* to determine their COX-2 and 5-LOX inhibitory potencies. Standard compounds celecoxib (COX-2 inhibitor) and zileuton (5-LOX inhibitor) were evaluated in parallel. As summarized in Table 1, all of these compounds exhibited COX-2 and 5-LOX inhibitory activities. Among them, CA amides having a F or Br in the *para*-position of N-1 phenyl ring (R^1) exhibited potent COX-2 inhibitory activity (**17a-c** and **18** , IC_{50} = 0.12-0.17 μM) that compared favorably to the positive control celecoxib (IC_{50} = 0.14 μM). It is notable that substitution of R^1 with electron-withdrawing group enhanced the COX-2 inhibitory activity. For instance, the fluorin substituted compound **14a** exhibited potent COX-2 inhibition (IC_{50} = 0.18 μM) that was 5-fold more potent than **14b** with a hydrogen in R^1 position (IC_{50} = 0.92 μM). In addition, the hybride compounds linking with amide linkage were more potent in COX-2 inhibition than those linking with ester-bounds. Meanwhile, the compounds substituting R^4 with a hydroxyl group exhibited potent 5-LOX inhibitory activity (**15a-e**, **18** and **22a-b**, IC_{50} = 0.71-0.87 μM) comparable to that of Zileuton (IC_{50} = 0.80 μM), which was consistent with reported conclusion that the hydroxyl group in R^4 position of CA is necessary for the inhibitory effect on 5-LOX [30]. The R^3 substituents also affected the 5-LOX inhibition slightly (5-LOX inhibition: OH, OCH3 > OAc > H). The structure-activity relationship was

summarized in Fig. 3. Based on the favorable results of COX-2 and 5-LOX inhibition, compounds **18**, **15c**, **22b** and **23a** were chosen to evaluate the selectivity between COX-1 and COX-2. The experiments suggested that these compounds showed good COX-1/COX-2 selectivity (Table 2).

Table 1. COX-2 and 5-LOX inhibitory activities of target compounds

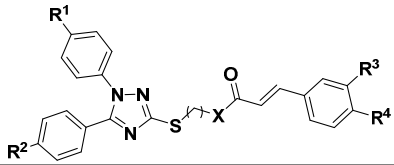

14a-d, 14g, 14i, 14k, 14m, 14o; 15a-e; 17a-c, 17e, 17g; 18; 21a-e; 22a-b; 23a, 23c

Compd.	R^1	R^2	n	X	R^3	R^4	COX-2 IC_{50} (μM)[a]	5-LOX IC_{50} (μM)[a]
14a	F	CH_3SO_2	2	O	OAc	OAc	0.18±0.03	1.05±0.21
14b	H	CH_3SO_2	2	O	OAc	OAc	0.92±0.15	1.21±0.19
14c	CF_3	CH_3SO_2	2	O	OAc	OAc	0.19±0.02	1.06±0.32
14d	Br	CH_3SO_2	3	O	OAc	OAc	0.29±0.04	0.99±0.08
14g	Br	NH_2SO_2	2	O	OAc	OAc	0.31±0.13	1.05±0.14
14i	F	NH_2SO_2	2	O	OAc	OAc	0.39±0.04	1.06±0.23
14k	H	NH_2SO_2	2	O	OAc	OAc	0.85±0.16	1.11±0.17
14m	F	NH_2SO_2	3	O	OAc	OAc	0.36±0.02	1.03±0.34
14o	H	NH_2SO_2	3	O	OAc	OAc	0.91±0.17	1.07±0.12
15a	H	CH_3SO_2	2	O	OH	OH	0.67±0.12	0.85±0.23
15b	Br	CH_3SO_2	3	O	OH	OH	0.37±0.04	0.79±0.18
15c	F	CH_3SO_2	3	O	OH	OH	0.18±0.06	0.71±0.09
15d	H	NH_2SO_2	2	O	OH	OH	0.62±0.07	0.80±0.14
15e	H	NH_2SO_2	3	O	OH	OH	0.64±0.16	0.77±0.08
17a	F	CH_3SO_2	2	NH	OAc	OAc	0.16±0.09	0.95±0.16
17b	Br	CH_3SO_2	3	NH	OAc	OAc	0.24±0.05	0.99±0.16
17c	F	CH_3SO_2	3	NH	OAc	OAc	0.17±0.01	0.98±0.08
17e	Br	NH_2SO_2	2	NH	OAc	OAc	0.18±0.02	0.99±0.15
17g	H	NH_2SO_2	3	NH	OAc	OAc	0.63±0.11	0.97±0.19
18	F	CH_3SO_2	3	NH	OH	OH	0.12±0.03	0.71±0.17
21a	Br	CH_3SO_2	2	O	OCH_3	OAc	0.29±0.05	0.94±0.21
21b	F	CH_3SO_2	2	O	OCH_3	OAc	0.24±0.01	0.92±0.19
21c	CH_3	CH_3SO_2	2	O	OCH_3	OAc	0.87±0.08	0.98±0.36
21d	H	CH_3SO_2	2	O	OCH_3	OAc	0.62±0.23	0.96±0.19
21e	CF_3	CH_3SO_2	2	O	OCH_3	OAc	0.23±0.06	0.92±0.06
22a	H	CH_3SO_2	2	O	OCH_3	OH	0.58±0.17	0.84±0.05
22b	CF_3	CH_3SO_2	2	O	OCH_3	OH	0.21±0.05	0.81±0.14
23a	Br	CH_3SO_2	3	O	H	H	0.42±0.04	1.30±0.25
23c	Br	NH_2SO_2	2	O	H	H	0.67±0.17	1.28±0.12
Celecoxib							0.14±0.03	—
Zileuton							—	0.80±0.07

[a] Values are means of four determinations.

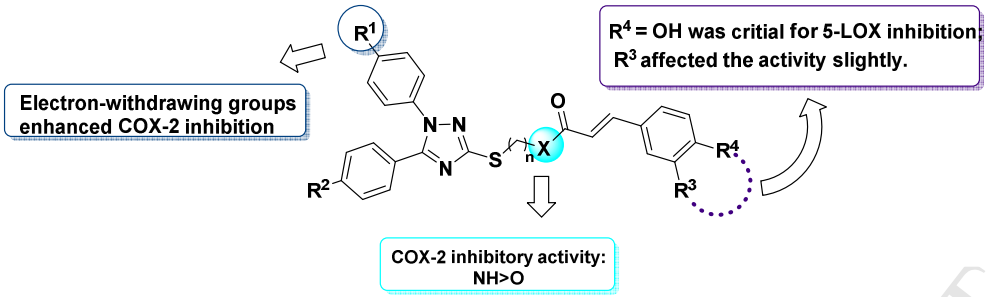

Fig. 3. Structure-activity relationships of hybrids of CA and diaryl-1.2.4-triazoles.

Table 2. *In vitro* COX-1/COX-2 inhibitory activity for compounds **18**, **15c**,**22b**,**23a**

Compd.	IC_{50} (μM) [a]		Selectivity Index [b] (SI)
	COX-1	COX-2	
15c	12.6±1.07	0.18±0.06	0.014
18	13.2±0.45	0.12±0.03	0.009
22b	20.5±1.52	0.21±0.05	0.010
23a	45.7±3.61	0.42±0.04	0.009
Celecoxib	8.2±0.69	0.14±0.03	0.017

[a]The test compound concentration required to produce 50% inhibition of COX-1/COX-2 is the mean of four determinations.

[b]*In vitro* COX-2 selectivity index (COX-2 IC_{50} / COX-1 IC_{50}).

2.3 Molecular modeling (docking) studies

To investigate the binging interactions, molecular docking studies were carried out between the most potent compound **18** which exhibited balanced COX-2/5-LOX inhibitory activities and the mammalian COX-2 and 5-LOX enzymes. The COX active site has been detailedly described with high-resolution structural information on COX-inhibitor complexes [37-39]. It consists of a long narrow hydrophobic channel extending from the membrane-binding domain to the heme cofactor. Despite their similarity, Ile in COX-1 is exchanged for Val in COX-2 at positions 434 and 523, which opens an side pocket off the main channel [40, 41]. Another essential factor for selectivity is Arg-513 in the side pocket, in place of a His in COX-1 [41]. As illustrated in Fig. 4 a) and b), the C-5 *p*-CH_3SO_2-phenyl moiety inserts into the side pocket, which is crucial for COX-2 selectivity. Moreover, the two oxygen atoms of SO_2CH_3 form hydrogen bonds with Arg-513 (NH···O,*d* = 2.4 Å) and His-89 (NH···O,*d* = 2.1 Å), increasing the stability of the complex. On the other hand, the fluoro-substituted phenyl is oriented towards the hydrophobic channel formed by Phe-518, Trp-387, Leu-352, Tyr-385 and Tyr-348. These interactions seem critical to the optimal inhibition of the enzyme. Besides, the secondary amine of the amide in linkage offers hydrogen bond to the oxygen atom of Tyr-355 (NH···O,*d* = 2.4 Å), which may contribute to the increase of COX-2 inhibitory activity upon replacing the ester to amide (e.g. **15c** COX-2 IC_{50} = 0.29 μM; **18** COX-2 IC_{50} = 0.12 μM).

Although the crystal structure of human 5-LOX has been reported in 2011 [42], it only gave an apo-structure with no inhibitor binding. And docking studies with known 5-LOX inhibitors showed that the correlation coefficient between the predicted and experimental IC_{50} was negative, reveling the crystal structure may not be used directly for drug design [43]. Hence 5-LOX

comparative model was built on the closed model of rabbit 15-LOX (PDB entry 2P0M, chain B, identity 38.6%) and coral 8*R*-LOX (PDB entry 2FNQ, identity 38.8%) for studying [43]. As shown in Fig 4 c) and d), the compound **18** is positioned in the center of the active site. The 4-fluoro phenyl is buried deep into the bottom channel of the hydrophobic pocket formed by Leu-368, His-372, Leu-414 and Phe-421, and the fluoro atom forms a hydrogen bond with His-372 (NH···F,*d* = 2.2 Å). Notably, the *para*-hydroxyl of CA could form hydrogen bond with Asn-180 (OH···O,*d* = 2.3 Å), which may result in the increase of 5-LOX inhibitory activity. The other three hydrogen bonds formed with Asn-180 (NH···O,*d* = 2.8 Å), Gln-413 (NH···O,*d* = 2.4 Å) and Asn-425 (NH···O,*d* = 2.3 Å) also play important role in 5-LOX inhibition. Altogether, the representative compound **18** binds with both active sites of COX-2 and 5-LOX via hydrophobic interactions. And the binding conformation is stabilized by hydrogen bonds. These docking studies revealed possible binding mode of these compounds, which may provide insight into the further modification of the hybrids of CA and diaryl-1.2.4-triazoles as COX-2/5-LOX dual inhibitors.

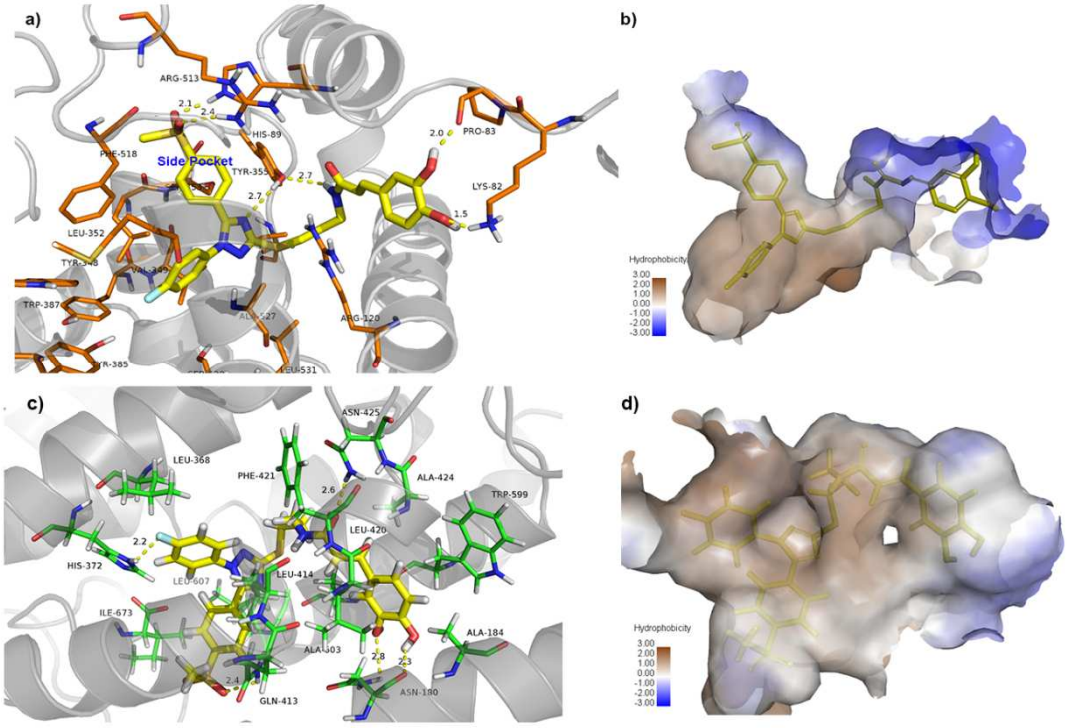

Fig. 4. Docking of compound **18** into the COX-2 (entry code: 4FM5) and 5-LOX (comparative model, templet: 15-LOX: 2P0M and 8*R*-LOX: 2FNQ) active site. a) H bonding interaction between **18** and COX-2; b) Hydrophobicity of the active site of COX-2; c) H bonding interaction between **18** and 5-LOX; d) Hydrophobicity of the 5-LOX pocket. Yellow lines represent hydrogen bonds.

2.4 MTT assay

According to COX-2/5-LOX inhibitory activities and structural characteristics, 22 compounds were selected for *in vitro* antiproliferative activity determination using MTT assay against four different cell lines (A549: human lung cancer, Caco-2: human colon cancer, PC-3: human prostate cancer and B16-F10: murine melanoma). Assays with cisplatin (CDDP), CAPE,

CA and compound **1** as reference compounds were included for comparison. As shown in Table 3, most test compounds showed potent inhibitory effects against these four cell lines, superior to the parent compounds (CA and compound **1**) and almost equivalent to CAPE. And the most potent compound **22b** exhibited equivalent antiproliferative activity to that of CDDP (IC_{50}: 6.78~9.05 μM of **22b** *vs*. 6.93~9.71 μM of CDDP). Interestingly, the amide derivatives **17a-c**, **17e**, **17g** and **18** with superior COX-2 inhibition activities showed weaker effect than ester derivatives on cell growth (*e.g.* COX-2: 0.12 μM of **18** *vs.* 0.29 μM of **15c**; cellular activity: 18.72~23.09 μM of **18** *vs.*9.52~11.16 μM of **15c**). It may result from the hydrophobicity of the compounds which may affect the drug permeation through biological membrane. Moreover, we found that the antiproliferative activity would increase as the *para*-position of N-1 phenyl ring (R^1) was substituted with electron withdrawing groups.

Table 3. Antiproliferative activities of selected compounds against different cancer cell lines.

Compd.	Cell lines (IC_{50}[a,b], μM ± SD)			
	A549	Caco-2	PC-3	B16-F10
CDDP[c]	6.93±0.01	9.20±0.23	7.69±0.04	9.71±0.11
CAPE	9.72±0.09	11.35±0.14	10.15±0.29	10.68±0.06
CA	>100	>100	>100	>100
1	29.53±0.31	41.25±0.24	37.47±0.53	32.28±0.17
14a	11.78±0.83	12.81±0.36	15.65±0.77	14.21±0.92
14c	10.19±0.15	11.30±0.27	14.51±0.13	11.46±0.33
14d	12.86±0.05	11.71±0.09	14.88±0.53	12.84±1.2
14i	12.04±0.11	10.97±0.32	9.84±0.47	11.03±0.15
14m	9.92±0.22	11.45±0.19	10.52±0.38	10.90±0.26
15a	13.80±0.49	14.75±0.23	14.56±0.12	14.97±0.44
15b	11.19±3.16	12.42±0.19	12.35±4.08	13.13±2.16
15c	9.52±3.16	11.16±0.19	10.11±4.08	10.43±2.16
15d	14.07±0.37	15.01±0.40	15.02±0.24	14.98±0.52
17a	17.01±0.35	15.08±0.41	18.03±0.63	14.62±0.19
17b	23.30±0.18	26.14±0.62	23.90±0.21	16.37±0.21
17c	21.82±0.12	20.77±0.85	17.56±0.13	15.23±0.12
17e	18.74±0.97	16.71±1.31	17.04±0.29	15.16±0.43
17g	32.72±1.26	31.03±1.74	35.21±1.56	29.06±1.31
18	22.14±0.13	20.92±0.26	23.09±0.15	18.72±0.19
21a	11.05±0.22	12.07±0.25	13.14±0.19	12.44±0.80
21b	9.61±0.14	10.81±0.36	12.77±0.21	11.18±0.43
21c	15.01±0.36	14.09±0.21	15.53±0.37	15.34±0.72
21e	9.65±0.17	10.77±0.41	9.81±0.73	10.47±0.11
22b	6.78±0.21	9.05±0.07	7.46±0.49	8.65±0.55
23a	22.34±0.31	24.56±0.09	21.92±1.61	19.44±0.51
23c	19.74±0.25	20.86±0.33	20.05±0.18	21.16±0.74

[a] IC_{50}: Concentration inhibits 50% of cell growth. [b] Results are expressed as the mean ± S.D. of three independent experiments. [c] CDDP: *cis*-Diammineplatinum(II) dichloride.

2.5 Induction of apoptosis by compound 15c

Considering the antiproliferative and COX-2/5-LOX inhibitory activity, the compound **15c** was selected for flow cytometry analysis. As shown in Fig. 5, compound **15c** could induce apoptosis in human non-small cell lung cancer A549 cells in a dose-dependent manner. Treatment of the A549 cells with compound **15c** at concentrations of 1 μM, 5 μM and 25 μM for 3 days resulted in cell apoptosis at ratios of 12.86%, 30.05% and 43.35% respectively, as compared with 7.51% in the vehicle control group.

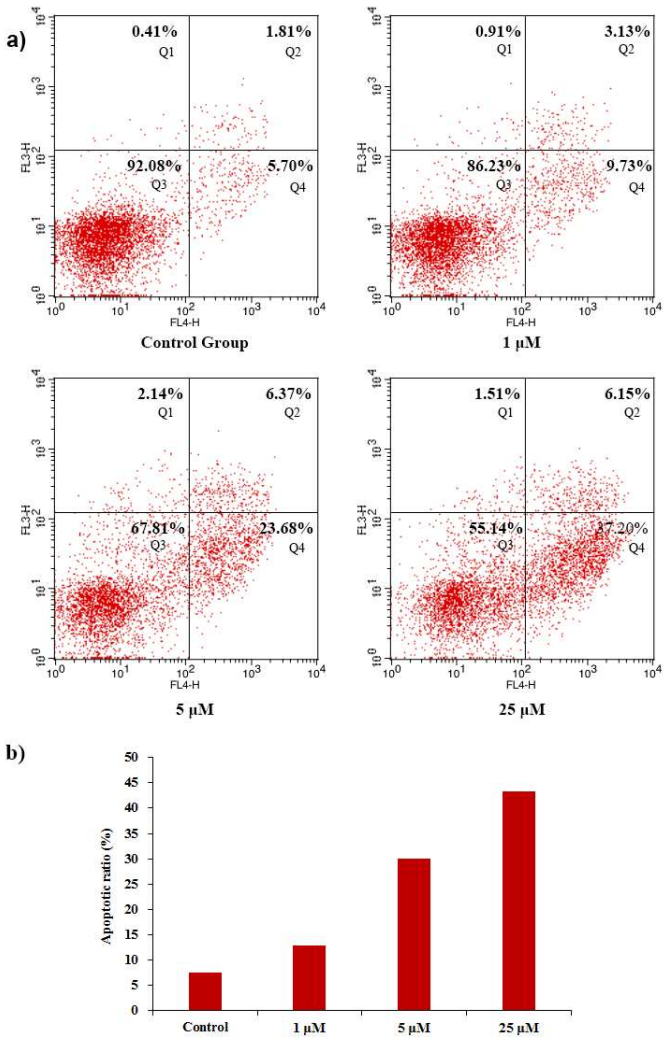

Fig. 5. Compound **15c** induces apoptosis in A549 cells. a): Flow cytometry analysis of apoptotic A549 cells; b): Apoptotic ratio.

2.6. Cell cycle studies of compound 15c

Furthermore, cell cycle progression experiments were designed to examine the cytostatic effects of **15c** on A549 cells. In control groups, the G1, S and G2 populations represented 54, 42 and 4% of the cells respectively. After incubation with **15c**, a G2-block was observed in a dose-dependent manner (Fig. 6). Similar results were reported by other researcher [40, 44].

Recently, Dong *et al.* [45] reported that EGFR and COX-2 were co-overexpressed and co-localized with each other and inhibition of COX-2 decreased levels of EGFR in cancer cells. And it is reported that inhibition of EGFR may give rise to G2/M phase cell cycle arrest [46, 47]. Taken together, It could suggest that the G2-block caused by compound **15c**, at least partially, assigned to its capacity to decrease EGFR expression. Although further experiments are needed to extend understanding of the mechanisms, these diaryl-1,2,4-triazole derivatives are expected to be promising candidates for the development of anticancer agents considering their remarkable biological profile and novel structure scaffold.

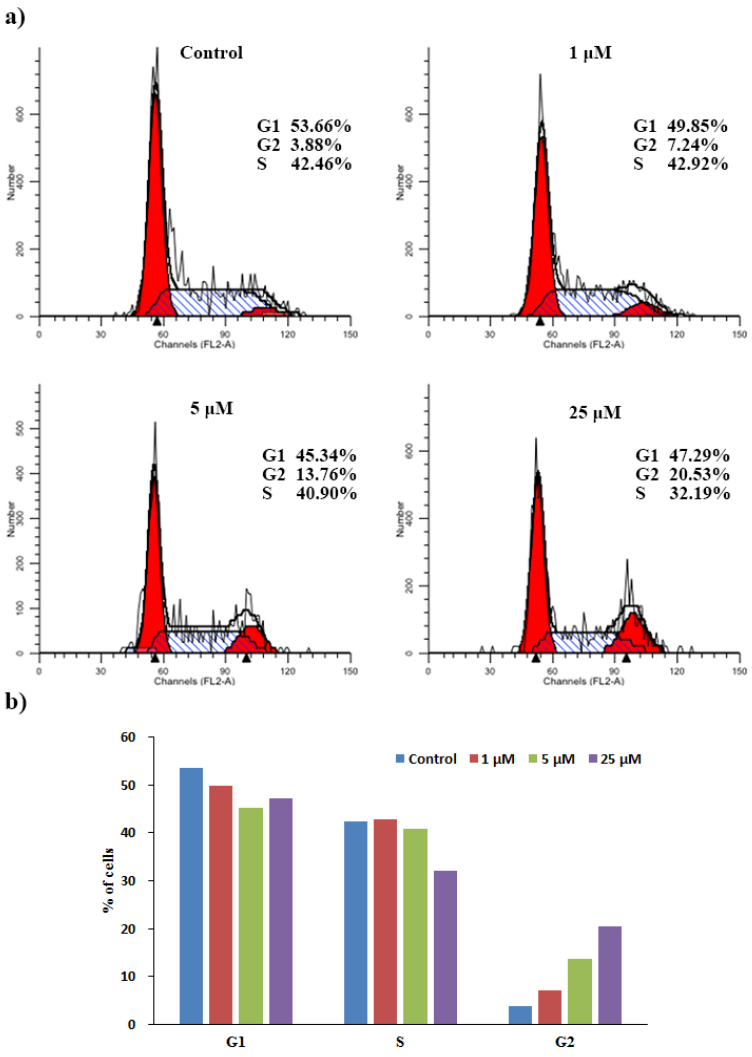

Fig. 6. Influence of compound **15c** on A549 cell cycle.

2.7 *In vivo* anti-tumor activity

Based on the results of cellar activities, we further tested the *in vivo* antitumor activity of the most potent compound **22b** against mice bearing B16-F10 melanoma. As illustrated in Table 4, **22b** inhibited the tumor growth in ratio of 58.9% at the dose of 40 mg/kg exhibiting potent antitumor activity. Preliminary biological evaluation *in vivo* indicated that compound **22b** was worthy of further study as a potential lead for development of

COX-2/5-LOX dual inhibitors for cancer therapy.

Table 4. *In vivo* antitumor activity of compound **22b** against mice bearing B16-F10 melanoma.

Drugs	Dose	Number of mice		Weight of mice (g)		Weight of tumor X±SD (g)	Ratio of inhibition (%)	*P* value
		start	end	Start	End			
Saline	0.4 ml/mouse	10	10	18.4 ± 1.1	28.1 ± 1.7	1.92 ± 0.61		
22b	40 mg/kg	10	10	18.6 ± 0.5	26.3 ± 2.4	0.79 ± 0.29	58.9	< 0.01
5-FU[a]	20 mg/kg	10	10	18.7 ± 0.9	26.0 ± 3.3	0.61 ± 0.51	68.2	< 0.01

[a] 5-FU: 5-Fluorouracil.

3. Conclusion

In continuation of our endeavor for novel anticancer candidates, we designed a new class of COX-2/5-LOX dual inhibitors through a pharmacophore hybrid approach followed by SAR studies. Twenty-nine derivatives were synthesized by hybridizing diaryl-1,2,4-triazoles with CA scaffold. All target compounds exhibited potent COX-2/5-LOX inhibitory activities and the selected compounds **18**, **15c**, **22b** and **23a** displayed excellent COX-1/COX-2 selectivity. The docking studies revealed possible binding mode of these compounds, which may provide insight into the further modification. Antiproliferative activity evaluation suggested that most of these compounds process potent antiproliferative activities. In mechanistic studies, the representative compound **15c** was found to induce apoptosis and G2/M phase cell cycle arrest in human lung cancer A549. Moreover, *in vivo* anti-tumor efficiency evaluation showed that the most potent compound **22b** could significantly inhibit tumor growth in mice. Although detailed mechanisms remain to be elucidated, compound **22b** could warrant further optimization to find novel anti-tumor drug candidates.

4. Experimental section

4.1 Chemistry

Most chemicals and solvents were purchased from commercial sources. Further purification and drying by standard methods were employed when necessary. Melting points were determined on an XT-4 micro melting point apparatus and uncorrected. IR spectra were recorded in $CDCl_3$ or KBr pellets on a Nicolet Impact 410 spectrophotometer. ^{1}H NMR and ^{13}C NMR spectra were recorded with a Bruker AV-300 spectrometer in the indicated solvents (TMS as internal standard): the values of the chemical shifts are expressed in δ values (ppm) and the coupling constants (*J*) in Hz. Purity of all tested compounds was ≥95%, as estimated by HPLC analysis. The major peak of the compounds analyzed by HPLC accounted for ≥95% of the combined total peak area when monitored by a UV detector at 210 nm. EI-MS spectra were recorded on an Agilent1100-

LC-MSD-Trap/SL spectrometer and High-resolution mass spectra were recorded using an Agilent QTOF 6520.

4.1.1 General procedure for synthesis of compounds 7a–f. The compound **6a-b, d, g** (1.46 mmol) and K_2CO_3 (1.46 mmol) were suspended in anhydrous acetone(12 mL) . The reaction mixture was stirred for 0.5 h at 50 ^oC, then ethyl bromoacetate or ehthyl 3-bromopropionate (2.08 mmol) was added and heat under reflux for 3 h. The reaction solution was then cooled down, filtered and concentrated under reduced pressure. The residue was brown oil and purified by silica gel column chromatography using petroleum ether/Ethyl acetate (3/1, V/V) to give **7a-f** (66-88% yield) as a white solids.

4.1.2 General procedure for synthesis of compounds 8a–f. To a solution of acetate **7a-f** (0.67 g, 1.35 mmol) in dry DMF (13 mL) was added LAH (0.102 g, 2.68 mmol) in batches at room temperature in 30 min, and heated under reflux for 3 h. Then the reaction mixture was cooled to room temperature and 6 mL ethyl acetate and 6 mL water were added. The layers were allowed to separate and the aqueous layer was extracted three times with ethyl acetate. The organic layer was combined, washed with a saturated sodium chloride aqueous solution and dried over anhydrous sodium sulfate then concentrated under reduced pressure. The residue purified by silica gel column chromatography using petroleum ether/ ethyl acetate (3/1, V/V) as eluent to give **8a-f** (50-78% yield) as solids.

4.1.3 General procedure for synthesis of compounds 9a–e. To a solution of **8a-e** (0.24 mmol) in dry dichloromethane (5 mL) were added TEA (0.091 mL, 0.66 mmol) and methylsulfonyl chloride (0.055 mL, 0.71 mmol) dropwise under ice bath and stirred for 2 h. The reaction mixture was diluted with dichloromethane and washed with water twice. The organic layer was dried over anhydrous sodium sulfate then concentrated under reduced pressure. The obtained colorless oil was purified by silica gel column chromatography using petroleum ether/ethyl acetate (3/1, V/V) as eluent to give **9a-e** (69-87% yield) as solids.

4.1.4 General procedure for synthesis of compounds 10a-e. To a solution of sulfonate **9a-e** (0.26 mmol) in dry DMF (10 mL) was added sodium azide (0.044 g, 0.68 mmol), then heat to 90 ^oC for 3 h. The reaction mixture was cooled to room temperature and extracted with ethyl acetate three times. The organic layer was combined and washed with saturated sodium chloride aqueous solution, then dried over anhydrous sodium sulfate and concentrated under reduced pressure. The obtained yellow oil was purified by silica gel column chromatography using petroleum ether/ ethyl acetate (4/1, v/v) as eluent to give **10a-e** (67-89% yield) as solids.

4.1.5 General procedure for synthesis of compounds 11a-e. To a solution of **10a-e** (0.25 mmol) in THF (5 mL) was added triphenylphosphine (0.399 g, 1.52 mmol). The mixture was stirred at room temperature overnight, then concentrated under reduced pressure. The residue was diluted with 5 mL of dichloromethane, then was washed with water and saturated sodium chloride aqueous solution successively. The organic layer was dried over anhydrous sodium sulfate and concentrated under reduced pressure. The obtained crude product was purified by silica gel column chromatography using dichloromethane/methanol/triethylamine (150/1/0.05, v/v/v) as eluent to give **11a-e** (57-80% yield) as solids.

4.1.6 Procedure for synthesis of compound 12(*(E)-3-(3,4- diacetoxyphenyl) acrylic acid***).**To a solution of CA (0.122 g, 0.68 mmol) suspended in dichloromethane (10 mL), DMAP (0.015 g, 0.12 mmol) was added. The reaction mixture was heated to reflux, and Ac_2O (0.20 mL, 2.13 mmol) and TEA (0.29 mL, 2.09 mmol) were added dropwise 5 min later, then refluxed for 4

h. The mixture was concentrated under reduced pressure and diluted with dichloromethane, then washed successively with 1N HCl, water and saturated sodium chloride aqueous solution. The organic layer was dried over anhydrous sodium sulfate and concentrated under reduced pressure. The obtained white solid was purified by silica gel column chromatography using dichloromethane/methanol (100/1, v/v) as eluent to give **12** (0.149 g, 83.3% yield) as a white solid. ESI-MS *m/z*: 265.1 $[M+H]^+$.

4.1.7 General procedure for synthesis of compounds 13a, b. To a solution of **12** (0.919 g, 3.48 mmol) suspended in dry acetone (25 mL) were added TEA (1.45 mL, 10.4 mmol) and 1,2-dibromoethane (0.90 mL, 10.4 mmol) or 1,3-dibromopropane dropwise at room temperature. The reaction mixture was heated to reflux and stirred for 24 h and then filtered. The filtrate was concentrated under reduced pressure. The residue was purified by silica gel column chromatography using petroleum ether/ethyl acetate (5/1, v/v) as eluent to give **13a,b** (31.8% and 42.6% yield respectively) as white solids.

4.1.8 General procedure for synthesis of compounds 14a-f, 14h, 14j, 14l and 14n. To a solution of **13a** or **13b** (0.27 mmol) in dry acetone (8 mL) were added K_2CO_3 (0.045 g, 0.33 mmol) and **6a-b**, **6d-e** or **6g-I** (0.30 mmol). The reaction mixture was stirred for 8 h at room temperature then filtered. The filtrate was concentrated under reduced pressure and the residue was purified by silica gel column chromatography using dichloromethane/methanol (300/1, v/v) as eluent to give **14a-f, 14h, 14j, 14l and 14n** (26-53% yield) as white solids or colorless oils.

(*E*)-4-(3-(2-((1-(4-fluorophenyl)-5-(4-(methylsulfonyl)phenyl)-1*H*-1,2,4-triazol-3 -yl)thio)ethoxy)-3-oxoprop-1-en-1-yl)-1,2-phenylene diacetate (**14a**) m.p. 66-70 ^oC. ^1H-NMR ($CDCl_3$, 300 MHz) *δ*: ppm 7.91 (2H, d, *J* = 8.3 Hz, Ar*H*), 7.67 (2H, d, *J* = 8.3 Hz, Ar*H*), 7.59 (1H, d, *J* = 17.6 Hz, -C*H*=), 7.25～7.34 (4H, m, Ar*H*), 7.11～7.22 (3H, m, Ar*H*), 6.35 (1H, d, *J* = 16.0 Hz, -C*H*=), 4.58 (2H, t, *J* = 6.4 Hz, OCH_2), 3.53 (2H, t, *J* = 6.4 Hz, SCH_2), 3.06 (3H, s, SO_2CH_3), 2.30 (6H, s, OAc); ^{13}C NMR (75 MHz, $CDCl_3$) *δ:* 168.02, 166.23, 164.45, 161.79, 161.24, 153.07, 142.15, 141.64, 139.35, 139.24, 133.59, 133.55, 131.76, 129.63, 127.76, 127.32, 127.20, 126.63, 125.85, 122.31, 121.98, 117.05, 116.74, 114.88, 63.51, 44.17, 33.85, 20.59, 20.56; IR (KBr, cm^{-1}) : 3462, 3134, 1774,1710, 1638, 1511, 1400, 1317, 1206, 1150, 1091, 988, 849, 780, 544; ESI-MS *m/z*: 640.1 $[M+H]^+$; HRMS (ESI): Calculated for $C_{30}H_{27}FN_3O_8S_2^+$ $[M+H]^+$: 640.1218, found: 640.1210.

4.1.9 General procedure for synthesis of compounds 14g, 14i, 14k, 14m, and 14o. To a solution of **14f**, **14h**, **14j**, **14l** or **14n** (0.13 mmol) in TFA (3 mL) were added 3 drops of anisole under ice bath. The reaction mixture was slowly heated to room temperature and stirred for 24 h. The mixture was concentrated under reduced pressure. The obtained residue was purified through silica gel column chromatography using dichloromethane/methanol (300/1, v/v) as eluent to give **14g, 14i, 14k, 14m** and **14o** (28-53% yield) as white solids.

4.1.10 General procedure for synthesis of compounds 15a-e, 18, 22a-b. To a solution of **14b-e, 14k, 14o, 17c, or 21d-e** (0.17 mmol) in methanol (3 mL) was added 30% sodium methylate MeOH solution dropwise until the PH value to 9. The reaction mixture was stirred at room temperature for 15 min then concentrated. Hydrochloric acid (10%) was added to give pH 5~6. The mixture was concentrated under reduced pressure and diluted with water (15 mL), then extracted with dichloromethane (10 mL×3) and washed with a saturated aqueous solution of sodium chloride. The organic layer was dried over anhydrous sodium sulfate and concentrated under reduced pressure. The residue was purified by silica gel column chromatography using

dichloromethane/methanol (100/1, v/v) as eluent to give target compounds (37-47% yield) as white or yellow solids.

(*E*)-2-((5-(4-(methylsulfonyl)phenyl)-1-phenyl-1H-1,2,4-triazol-3-yl)thio)ethyl 3-(3,4-dihydroxyphenyl)acrylate (**15a**): m.p. 196-198 ^{o}C. ^{1}H-NMR (DMSO-*d6*, 300 MHz) δ: ppm 9.62 (1H, s, O*H*), 9.14 (1H, s, O*H*), 7.92 (2H, d, *J* = 8.5 Hz, Ar*H*), 7.64 (2H, d, *J* = 8.5 Hz, Ar*H*), 7.45 (1H, d, *J* = 15.6 Hz, -C*H*=), 7.46～7.51 (3H, m, Ar*H*), 7.39～7.46 (2H, m, Ar*H*), 7.00 (1H, s, Ar*H*), 6.96 (1H, d, *J* = 8.1 Hz, Ar*H*), 6.73 (1H, d, *J* = 8.0 Hz, Ar*H*), 6.22 (1H, d, *J* = 15.9 Hz, -C*H*=), 4.47 (2H, t, *J* = 5.9 Hz, OCH_2), 3.51 (2H, t, *J* = 5.8 Hz, SCH_2), 3.25 (3H, s, CH_3SO$_2$); ^{13}C NMR (75 MHz, DMSO-d_6) δ 166.66, 160.04, 153.56, 148.93, 146.00, 145.91, 142.49, 137.56, 132.08, 130.08, 130.04, 129.97, 127.59, 126.15, 125.81, 121.88, 116.15, 115.25, 113.93, 63.04, 43.61, 30.49; IR (KBr, cm^{-1}): 3415, 3133, 2360, 1628, 1517, 1499, 1400, 1290, 1142, 1086, 996, 857, 820, 735, 528; ESI-MS m/z: 538.1 [M+H]$^+$; HRMS (ESI): Calculated for $C_{26}H_{24}N_3O_6S_2^+$ [M+H]$^+$: 538.1101, found: 538.1103.

(*E*)-3-(3,4-dihydroxyphenyl)-*N*-(3-((1-(4-fluorophenyl)-5-(4-(methylsulfonyl)ph-enyl)-1*H*-1,2,4-triazol-3-yl)thio)propyl)acrylamide (**18**): m.p. 80-82 ^{o}C; ^{1}H-NMR (DMSO-d_6, 300 MHz) δ: ppm 9.21 (2H, brs, O*H*), 8.09 (1H, t, *J* = 5.2 Hz, N*H*), 7.94 (2H, d, *J* = 8.6 Hz, Ar*H*), 7.68 (2H, d, *J* = 8.6 Hz, Ar*H*), 7.51～7.59 (2H, m, Ar*H*), 7.33～7.39 (2H, m, Ar*H*), 7.23 (1H, d, *J* = 15.7 Hz, -C*H*=), 7.93 (1H, s, Ar*H*), 6.82 (1H, d, *J* = 8.3 Hz, Ar*H*), 6.74 (1H, d, *J* = 8.0 Hz, Ar*H*), 6.30 (1H, d, *J* = 15.8 Hz, -C*H*=), 3.67 (2H, t, *J* = 6.6 Hz, SCH_2), 3.24 (3H, s, SO$_2$CH_3), 3.17 (2H, t, *J* = 5.8 Hz, NHCH_2); ^{13}C NMR (75 MHz, DMSO) δ: 167.70, 164.61, 161.41, 152.84, 145.96, 143.64, 140.59, 139.62, 133.73, 129.69, 129.47, 127.88, 127.46, 127.34, 124.71, 122.16, 122.12, 121.78, 118.73, 116.90, 116.59, 115.43, 44.17, 40.21, 32.42, 29.60. IR (KBr, cm^{-1}): 3458, 3135, 1655, 1510, 1400, 1262, 1147, 1090, 989, 843, 804, 776, 541; ESI-MS *m/z*: 569.2 [M+H]$^+$; HRMS (ESI): Calculated for $C_{27}H_{25}FN_4NaO_5S_2^+$ [M+Na]$^+$: 591.1149, found: 591.1158.

(E)-2-((5-(4-(methylsulfonyl)phenyl)-1-phenyl-1H-1,2,4-triazol-3-yl)thio)ethyl 3-(4-hydroxy -3-methoxyphenyl)acrylate (**22a**): m.p. 94-98 ^{o}C; ^{1}H-NMR (CDCl3, 300 MHz) δ: ppm 7.86 (2H, d, *J* = 8.5 Hz, Ar*H*), 7.67 (2H, d, *J* = 8.5 Hz, Ar*H*), 7.60 (1H, d, *J* = 15.9 Hz, -C*H*=), 7.44～7.47 (3H, m, Ar*H*), 7.30～7.33 (2H, m, Ar*H*), 6.99～7.04 (2H, m, Ar*H*), 6.89 (1H, d, *J* = 8.1 Hz, Ar*H*), 6.28 (1H, d, *J* = 15.9 Hz, -C*H*=), 5.96 (1H, s, O*H*), 4.58 (2H, t, *J* = 6.4 Hz, OCH_2), 3.90 (3H, s, OCH_3), 3.54 (2H, t, *J* = 6.4 Hz, SCH_2), 3.06 (3H, s, SO$_2$CH_3); ^{13}C NMR (75 MHz, CDCl$_3$) δ 166.85, 160.87, 152.86, 148.04, 146.74, 145.24, 141.74, 137.35, 132.44, 129.71, 129.66, 129.55, 127.57, 126.82, 125.31, 123.05, 114.99, 114.69, 109.36, , 62.98, 55.92, 44.28, 30.52; IR (KBr, cm^{-1}): 3454, 3143, 1693, 1637, 1604, 1515, 1501, 1400, 1309, 1286, 1267, 1147, 1092, 780, 698, 599, 578, 531; ESI-MS m/z: 552.1 [M+H]$^+$; HRMS (ESI): Calculated for $C_{27}H_{26}N_3O_6S_2^+$ [M+H]$^+$: 552.1258, found: 552.1261.

4.1.11 Procedure for synthesis of compound 16(*(E)-3-(3,4- diacetoxyphenyl) acryloyl chloride***).** To a solution of acid **12** (0.220 g, 0.83 mmol) in thionyl chloride (8mL) was added one drop of DMF as catalyst. The mixture was heated to reflux for 3 h, then was concentrated under reduced pressure to give 16 (0.219 g, 93.0% yield) as a brownness solid. ESI-MS *m/z*: 282.0 [M+H]$^+$.

4.1.12 General procedure for synthesis of compounds 17a-d, 17f. To a solution of amine **11a-e** (0.38 mmol) in dry DMF (7 mL) were added TEA (0.078 mL, 0.56 mmol) and **16** (0.156 g, 0.56 mmol) under ice bath. The reaction mixture was slowly heated to room temperature and stirred for another 8 h. The mixture was diluted with dichloromethane, then washed with water

and saturated aqueous solution of sodium chloride successively. The organic layer was dried over anhydrous sodium sulfate and concentrated under reduced pressure. The obtained yellow oil was purified by silica gel column chromatography (eluent: dichloromethane/methanol = 200:1) to give **17a-d** or **17f** (37-76% yield) as white or yellow solids.

(*E*)-4-(3-((2-((1-(4-fluorophenyl)-5-(4-(methylsulfonyl)phenyl)-1*H*-1,2,4-triaz-ol-3-yl-)thio)ethyl)amino)-3-oxoprop-1-en-1-yl)-1,2-phenylene diacetate (**17a**): m.p. 80-84 ^{o}C. ^{1}H-NMR ($CDCl_3$, 300 MHz) δ: ppm 7.88 (2H, d, J = 8.4 Hz, Ar*H*), 7.55 (2H, d, J = 8.3 Hz, Ar*H*), 7.25～7.29 (6H, m, Ar*H*, -C*H*=), 7.20 (3H, m, Ar*H*), 6.48 (1H, d, J = 15.9 Hz, -C*H*=), 3.67 (2H, m, SCH_2), 3.32 (2H, t, J = 5.9 Hz, NHCH_2), 3.06 (3H, s, SO_2CH_3), 2.25 (6H, s, OAc); ^{13}C NMR (75 MHz, $CDCl_3$) δ: 168.03, 165.53, 164.43, 161.22, 153.06,142.12, 141.62, 139.22, 139.10, 133.56, 131.91, 129.60, 127.75, 127.32, 127.20, 125.86, 123.82, 122.29, 121.64, 117.08, 116.77, 44.17, 40.13, 31.78, 20.61, 20.57; IR (KBr, cm^{-1}): 3461, 3133, 2925, 2854, 1774, 1637, 1510, 1400, 1206, 1106, 987, 841, 771, 544; ESI-MS m/z: 639.0 $[M+H]^+$; HRMS (ESI): Calculated for $C_{30}H_{27}FN_4NaO_7S_2^+$ $[M+Na]^+$: 661.1197, found: 661.1200.

4.1.13 General procedure for synthesis of compounds 17e, 17g ans 23c. To a solution of **17d** ,**17f** or **23b** (0.09 mmol) in TFA (2.5 mL) was added two drops of benzaldehyde under ice bath. The reaction mixture was slowly heated to room temperature and stirred for 24 h. Then the mixture was concentrated under reduced pressure. The obtained brownish red oil was purified by silica gel column chromatography using dichloromethane/methanol (150/1, v/v) as eluent to give **17e,17g** or **23b** (45-83% yield) as white bubble solids.

2-((1-(4-bromophenyl)-5-(4-sulfamoylphenyl)-1H-1,2,4-triazol-3-yl)thio)ethyl cinnamate (**23c**): m.p. 78-82 ^{o}C; ^{1}H-NMR ($CDCl_3$, 300 MHz) δ: ppm 7.86 (2H, d, J = 8.3 Hz, Ar*H*), 7.67 (1H, d, J = 16.0 Hz, -C*H*=), 7.52～7.59 (4H, m, Ar*H*, -C*H*=), 7.46～7.51 (2H, m, Ar*H*), 7.36～7.38 (3H, m, Ar*H*), 7.17 (2H, d, J = 8.6 Hz, Ar*H*), 6.40 (1H, d, J = 16.0 Hz, -C*H*=), 5.28 (2H, s, SO_2NH_2), 4.57 (2H, t, J = 6.3 Hz, OCH_2), 3.52 (2H, t, J = 6.3 Hz, SCH_2); ^{13}C NMR (75 MHz, $CDCl_3$) δ: 166.63, 161.12, 153.12, 145.25, 143.55, 136.28, 134.20, 132.86, 131.13, 130.41, 129.50, 128.88, 128.06, 126.78, 126.62, 125.31, 123.33, 117.58, 63.11, 30.41; IR (KBr, cm^{-1}): 3416, 3134, 1637, 1492, 1400, 1166, 1095, 986, 833, 767, 619, 543; ESI-MS m/z: 585.0 [M+H]+; HRMS (ESI): Calculated for $C_{25}H_{22}BrN_4O_4S_2^+$ $[M+H]^+$: 585.0260, found: 585.0268.

4.1.14 Procedure for synthesis of compound 19 (*(E)-3-(4-acetoxy-3-methoxyphenyl)acrylic acid***).** To a solution of ferulic acid (0.490 g, 2.52 mmol) suspended in acetic anhydride (5 mL) was added one drop of concentrated sulfuric acid. The reaction mixture was stirred 12 minutes at room temperature. The mixture was poured into 5 mL of ice water to give white crystal, filtered and collected the solid . The residue was dissolved in saturated potassium carbonate solution and filtered again. 2N HCl was added to the filtrate to adjust the pH(≈4) and a lot of white solid was separated out. Then the mixture was filtered, and the residue was washed with water before drying to give **19** (0.536 g,89.9% yield) as a white solid.

4.1.15 Procedure for synthesis of compound 20 (*(E)-2-bromoethyl 3-(4-acetoxy-3-methoxyphenyl)acrylate***).** To a solution of **19** (0.536 g, 2.27 mmol) in dry acetone (6 mL) were added TEA (0.95 ml, 6.84 mmol) and 1,2-dibromoethane (0.59 ml, 6.85 mmol) . The reaction mixture was heated to reflux and stirred for another 24 h and filtered, then the filtrate was concentrated under reduced pressure to give brown oil residue. The residue was purified by silica gel column chromatography using petroleum ether/ ethyl acetate (5/1, v/v) as eluent to give **20** (0.481 g, 61.8% yield) as a white solid. ^{1}H-NMR ($CDCl_3$, 300 MHz) δ: ppm 7.69 (1H, d, J = 16.0

Hz, -C*H*=), 7.12～7.15 (2H, m, Ar*H*), 7.06 (1H, d, *J* = 7.9 Hz, Ar*H*), 6.41 (1H, d, *J* = 16.0 Hz, -C*H*=), 4.52 (2H, t, J = 6.1 Hz, OCH_2), 3.87 (3H, s, OCH_3), 3.59 (2H, t, *J* = 6.1 Hz, CH_2Br), 2.32 (3H, s, OAc); ESI-MS *m/z*: 362.4 $[M+NH_4]^+$.

4.1.16 General procedure for synthesis of compounds 21a-e. To a solution of **20** (0.100 g, 0.29 mmol) in dry acetone (8 mL) were added K_2CO_3 (0.048 g, 0.35 mmol) and **6a-c** or **6h-i** (3.49 mmol) . The reaction mixture was stirred for 5 h at room temperature then filtered. The filtrate was concentrated under reduced pressure to give brown bubble solid. The residue was purified by silica gel column chromatography using dichloromethane/methanol (300/1, v/v) as eluwnt to give **21a-e** (42-57% yield) as white solids.

(E)-2-((1-(4-bromophenyl)-5-(4-(methylsulfonyl)phenyl)-1H-1,2,4-triazol-3-yl)thio) ethyl 3-(4-acetoxy-3-methoxyphenyl)acrylate (**21a**): m.p. 160-164 ^oC. ^{1}H-NMR ($CDCl_3$, 300 MHz) δ: ppm 7.93 (2H, d, *J* = 8.3 Hz, Ar*H*), 7.56～7.69 (5H, m, Ar*H*, -C*H*=), 7.19 (2H, d, *J* = 8.6 Hz, Ar*H*), 7.02～7.06 (3H, m, Ar*H*), 6.36 (1H, d, *J* = 16.0 Hz, -C*H*=), 4.59 (2H, t, *J* = 6.2 Hz, OCH_2), 3.84 (3H, s, OCH_3), 3.53 (2H, t, *J* = 6.2 Hz, SCH_2), 3.07 (3H, s, SO_2CH_3), 2.32 (3H, s, OAc); ^{13}C NMR (75 MHz, $CDCl_3$) δ: 169.05, 166.76, 161.03, 152.96, 151.43, 146.06, 144.59, 141.85, 141.77, 133.23, 132.71, 132.53, 129.77, 128.82, 125.36, 122.67, 123.25, 121.36, 117.95, 111.30, 63.20, 56.07, 44.30, 30.42, 20.63; IR (KBr, cm-1): 3461, 3133, 2922, 2835, 1638, 1400, 1147, 1089, 988, 833, 780, 527; ESI-MS m/z: 672.0 [M+H]+; HRMS (ESI): Calculated for $C_{29}H_{27}BrN_3O_7S_2^+$ $[M+H]^+$: 672.0468, found: 672.0455.

4.1.17 General procedure for synthesis of compounds 23a-b. To a solution of **8b** or **8F** (0.40 mmol) in dry dichloromethane (12 mL) were added DCC (0.080 g, 0.58 mmol), DMAP (0.045 g, 0.37 mmol) and Cinnamic acid (0.072 g, 0.49 mmol) . The reaction mixture was stirred overnight at room temperature and filtered, then the filtrate was concentrated under reduced pressure.The residue was purified by silica gel column chromatography using petroleum ether/ ethyl acetate (3/1, v/v) as eluent to give **23a-b** (0.118 g, 49% and 53% yield respectively) as white solids.

3-((1-(4-bromophenyl)-5-(4-(methylsulfonyl)phenyl)-1H-1,2,4-triazol-3-yl)thio)propyl cinnamate (**23a**): m.p. 64-68 ^oC. ^{1}H-NMR ($CDCl_3$, 300 MHz) δ: ppm 7.91 (2H, d, *J* = 8.5 Hz, Ar*H*), 7.65～7.69 (3H, m, Ar*H*, -C*H*=), 7.55 (2H, d, *J* = 8.7 Hz, Ar*H*), 7.48～7.51 (2H, m, Ar*H*), 7.38～7.40 (3H, m, Ar*H*), 7.21 (2H, d, *J* = 11.5 Hz, Ar*H*), 6.41 (1H, d, *J* = 16.0 Hz, -C*H*=), 4.38 (2H, t, *J* = 6.1 Hz, OCH_2), 3.35 (2H, d, *J* = 6.2 Hz, SCH_2), 3.04 (3H, s, SO_2CH_3), 2.25 (2H, m, -CH_2-); ^{13}C NMR (75 MHz, $CDCl_3$) δ: 166.79, 161.56, 153.95, 144.99, 143.52, 141.69, 134.75, 132.57, 132.45, 129.97, 129.75, 129.51, 128.86, 126.38, 125.30, 122.83, 122.08, 63.85, 44.29, 29.75, 28.25; IR (KBr, cm^{-1}): 3418, 3134, 2927, 2852, 1637, 1492, 1400, 1312, 1148, 1089, 986, 837, 776, 597, 531, 484, 453, 433, 412; ESI-MS m/z: 598.1 $[M+H]^+$; HRMS (ESI): Calculated for $C_{27}H_{25}BrN_3O_4S_2^+$ $[M+H]^+$: 598.0464, found: 598.0470.

All the analytical data of other compounds are shown in supporting information.

4.2 *In vitro* COX and 5-LOX inhibition assay

The ability of the synthesized compounds to inhibit COX-1 was determined by 6-keto-$PGF_{1\alpha}$assay. Endotheliocyte was gained from the aorta pectoralis of neogenesis calf *in vitro*. The cells (1.0×10^6 cells) in 1 mL of DMEM supplemented with 10% heated-inactivated fetal

bovine serum, 2 mM glutamine, 60 mg/L penicillin and 100 mg/L streptomycin were plated in a 24-well culture plate and incubated at 37 ^{o}C under an atomosphere of 5% CO_2 for 24 h. Then the cells were treated with test compounds, DMSO and celecoxib, incubated for 20 min. Then arachidonic acid (10 μM) was added. After incubation for another 20 min, the culture was collected for 6-keto-PGF1α determination. 6-keto-PGF1α was measured by using a radioimmunity assay kit according to the manufacturer's instructions.

The COX-2 inhibitory activity was determined by PGE_2 production assay in rat abdominal macrophages. Cells in 1 mL of RPMI 1640 containing 5% FCS were plated in a 24-well plate at a density of 1.0×10^6cells per well. Incubated for 24 h at 37 ^{o}C under an atomosphere of 5% CO_2, then aspirin (1 mM) was added to inactivate COX-1. Replaced the culture media with fresh meida containing LPS (1 μg/mL) to induce COX-2 expression. After incubation for 6 h, the cell were treated with the test compounds , celecoxib and DMSO and incubated for 30 min. Added arachidonic acid (10 μM) and after incubation for another 20 min, the culture were collected for PGE_2 determination using an enzyme immunoassay (EIA) kit (Cat-lot no.414010, 96-well, Cayman Chemical Company) according to the manufacturer's instructions.

The inhibitory potency of target compounds on 5-LOX was determined by the production of LTB_4 under the stimulation of calcium ionophore A23187. Leukocytes were obtained from the abdominal cavity of Sprague-Dawley rats which have been injected intraperitoneally with 20 mL/kg of a 0.2% (w/v) glycogen solution. The cell suspensions were collected with Hanks solution and plated in a 24-well plate at the density of 1.0×10^6cells per well. After incubation for 10 min at 37 ^{o}C under an atomosphere of 5% CO_2, the cells were treated with *L*-cysteine (10 mM), indomethacin (1 mg/L), DMSO, celecoxib and test compounds in turn and incubated for another 30 min. Added calcium ionophore A23187 (5 μmol) to initiate LTB_4 production and incubated for another 30 min. After being clarified by centrifugation, the supernatant was plated in a 96-well plate and incubated overnight at 4 ^{o}C. Added chromogen and retained for 90 min. The 5-LOX activity was determined by using an EIA kit (Cat-lot no. 520111, 96-well, Cayman Chemical Company) according to the manufacturer's instructions. Percent inhibition was calculated according to the following formula:

Inhibition (%) = 100 × (OD blank – OD comp)/OD blank.

The IC_{50} values were determined as the maximal inhibition (100%) by Bliss method.

4.3 Molecular modeling (docking) study

Molecular docking studies with flexible ligand and rigid receptor were performed with the AutoDock Vina program[48]. Structures of the proteins and ligand were prepared using AutoDockTools GUI for docking preparation. The pictures were generated using Pymol and Discover Studio Visualizer 4.0 software. For COX-2, crystallographic structure in complex with (2-fluorobiphenyl-4-yl)acetic acid (PDB ID: 4FM5) were used for docking. The volume chosen for the grid box was 24 Å × 24 Å × 24 Å, center point (x = 19.137, y = -14.174, z = -46.89). Exhaustiveness was increase to 20, and 14 ligand poses were generated. The structure of 5-LOX was comparatively modeled as descriped in previous report [39]. The grid box was defined to include residues of the active site with the grid size of 24 Å × 26 Å × 26 Å. Exhaustiveness was increase to 20 and 9 ligand poses were generated.

4.4 MTT assay *in vitro*

Test cell lines were plated on 96-well plates at the density of 5×10^4/well and incubated for 24 h at 37 ^oC under an atomosphere of 5% CO_2. All of the test compounds were dissolved in DMSO at different concentrations and treated to the cells. Incubated for another 72 h following by the addition of MTT (5mg/mL in PBS), After incubating for 4 h, the optical density was detected with a microplate reader at 570 nm. The IC_{50} was calculated according to the dose-dependent curves and expressed as mean ± S.D. of three independent experiments.

4.5 Analysis of cellular apoptosis

A549 cells were seed into 6-well plates and incubated for 24 h at 37 ^oC under an atomosphere of 5% CO_2. Then test compounds were added in a certain concentration and negative control which was treated with DMSO were included. After incubation for 72 h, the treated cells were trypsinized. Washed the cells with PBS twice and centrifuged at 2000 rpm to collect the cells (5×10^5). 500 μL of binding buffer were added to suspend the cells. Then 5 μL of Annexin V-APC and 7-AAD were added successively and mixed well. Reacted for 5~15 min at room temperature in dark and analyzed the cell apoptosis with flow cytometry (FACS Calibur Bectone-Dickinson).

4.6 Analysis of cell cycle arrest

The A549 cells were incubated with the test compounds as described above. After incubating for 72 h, the treated cells were trypsinized, washed with PBS and centrifuged at 2000 rpm. The collected cells were fixed by adding cold ethanol (4 ^oC, overnight) and incubated for 30 min in PBS containing 100 μL RNase A of RNase and 400μL of propidium iodide. Cell DNA content was measured using flow cytometry (FACS Calibur Bectone-Dickinson) for cell cycle distribution analysis.

4.7 *In vivo* antitumor assay

Antitumor activity against mice bearing B16-F10 melanoma was performed as described by Cao *et al.* with a slight modification [49]. Mice (from Institute of Cancer Research) with body weight 18-22 g were transplanted with B16-F10 cells on the right oxter subcutaneously. 7 days later, mice were weighted and divided randomly in to 3 groups (10 mice/group). Treated the three groups of mice with saline (containing 1% DMSO/2% poloxamer, vehicle), test compound **22b** (40 mg/kg) and 5-FU (20 mg/kg, positive control) through intravenous injection respectively. The mice were sacrificed at the 25th day after tumor transplantation. Excised the tumors and weighted. The inhibition was calculated as follows: Tumor inhibition ratio (%) = (1-average tumor weight of the drug treated group/average tumor weight of vehicle group) × 100%.

Acknowledgement

This study was supported by the grants from State Key Laboratory of Natural Medicines, China Pharmaceutical University (No. SKLNMZZCX201404), Natural Science Foundation of Jiangsu Province (No. BK20130645), Huahai Pharmaceutical Graduate Innovation Fund (No. CX14B-005HH) and Innovation project of Jiangsu Province (No. KYLX15-0636). We appreciate Prof. Luhua Lai of Peking University for direction of comparative modeling of 5-LOX.

Conflicts of interest

The authors declare no conflict of interest.

Supporting Information

Detailed experimental procedures including spectroscopic and analytical data.

Reference:

[1] A. Mantovani, P. Allavena, A. Sica, F. Balkwill, Cancer-related inflammation, Nature, 454 (2008) 436-444.

[2] A. Mantovani, Cancer: inflaming metastasis, Nature, 457 (2009) 36-37.

[3] S.I. Grivennikov, F.R. Greten, M. Karin, Immunity, inflammation, and cancer, Cell, 140 (2010) 883-899.

[4] L.M. Coussens, L. Zitvogel, A.K. Palucka, Neutralizing tumor-promoting chronic inflammation: a magic bullet?, Science, 339 (2013) 286-291.

[5] S. Tavolari, M. Bonafè, M. Marini, C. Ferreri, G. Bartolini, E. Brighenti, S. Manara, V. Tomasi, S. Laufer, T. Guarnieri, Licofelone, a dual COX/5-LOX inhibitor, induces apoptosis in HCA-7 colon cancer cells through the mitochondrial pathway independently from its ability to affect the arachidonic acid cascade, Carcinogenesis, 29 (2008) 371-380.

[6] N. Ghosh, R. Chaki, V. Mandal, S.C. Mandal, COX-2 as a target for cancer chemotherapy, Pharmacol. Rep., 62 (2010) 233-244.

[7] A. Maitra, R. Ashfaq, C.R. Gunn, A. Rahman, C.J. Yeo, T.A. Sohn, J.L. Cameron, R.H. Hruban, R.E. Wilentz, Cyclooxygenase 2 expression in pancreatic adenocarcinoma and pancreatic intraepithelial neoplasia an immunohistochemical analysis with automated cellular imaging, Am. J. Clin. Pathol., 118 (2002) 194-201.

[8] H. Sano, Y. Kawahito, R.L. Wilder, A. Hashiramoto, S. Mukai, K. Asai, S. Kimura, H. Kato, M. Kondo, T. Hla, Expression of cyclooxygenase-1 and-2 in human colorectal cancer, Cancer Res., 55 (1995) 3785-3789.

[9] B. Rigas, I.S. Goldman, L. Levine, Altered eicosanoid levels in human colon cancer, J. Lab. Clin. Med., 122 (1993) 518-523.

[10] M. Mutoh, M. Takahashi, K. Wakabayashi, Roles of prostanoids in colon carcinogenesis and their potential targeting for cancer chemoprevention, Curr. Pharm. Des., 12 (2006) 2375-2382.

[11] S.M. Prescott, R.L. White, Self-promotion? Intimate connections between APC and prostaglandin H synthase-2, Cell, 87 (1996) 783-786.

[12] Y. Cao, A.T. Pearman, G.A. Zimmerman, T.M. McIntyre, S.M. Prescott, Intracellular unesterified arachidonic acid signals apoptosis, Proc. Natl. Acad. Sci. U. S. A., 97 (2000) 11280-11285.

[13] M.K. Saini, P. Sharma, J. Kaur, S.N. Sanyal, The cyclooxygenase-2 inhibitor etoricoxib is a potent chemopreventive agent of colon carcinogenesis in the rat model, J. Environ. Pathol. Toxicol. Oncol., 28 (2009).

[14] L. Wang, W. Chen, X. Xie, Y. He, X. Bai, Celecoxib inhibits tumor growth and angiogenesis in an orthotopic implantation tumor model of human colon cancer, Exp. Oncol., 30 (2008) 42-51.

[15] L.G. Melstrom, D.J. Bentrem, M.R. Salabat, T.J. Kennedy, X.-Z. Ding, M. Strouch, S.M. Rao, R.C. Witt, C.A. Ternent, M.S. Talamonti, Overexpression of 5-lipoxygenase in colon polyps and cancer and the effect of 5-LOX inhibitors in vitro and in a murine model, Clin. Cancer Res., 14 (2008) 6525-6530.

[16] S. Gupta, M. Srivastava, N. Ahmad, K. Sakamoto, D.G. Bostwick, H. Mukhtar, Lipoxygenase-5 is overexpressed in prostate adenocarcinoma, Cancer, 91 (2001) 737-743.

[17] Y.-N. Ye, E.S.-L. Liu, V.Y. Shin, W.K.-K. Wu, C.-H. Cho, Contributory role of 5-lipoxygenase and its association with angiogenesis in the promotion of inflammation-associated colonic tumorigenesis by cigarette smoking, Toxicology, 203 (2004) 179-188.

[18] I. Avis, S.H. Hong, A. Martínez, T. Moody, Y.H. Choi, J. Trepel, R. Das, M. Jett, J.L. Mulshine, Five-lipoxygenase inhibitors can mediate apoptosis in human breast cancer cell lines through complex eicosanoid interactions, FASEB J., 15 (2001) 2007-2009.

[19] M. Chatterjee, S. Das, K. Roy, M. Chatterjee, Overexpression of 5−lipoxygenase and its relation with cell proliferation and angiogenesis in 7, 12−dimethylbenz (α) anthracene−induced rat mammary carcinogenesis, Mol. Carcinog., 52 (2013) 359-369.

[20] L.T. Soumaoro, S. Iida, H. Uetake, M. Ishiguro, Y. Takagi, T. Higuchi, M. Yasuno, M. Enomoto, K. Sugihara, Expression of 5-lipoxygenase in human colorectal cancer, World J. Gastroenterol., 12 (2006) 6355-6360.

[21] A. Ihara, K. Wada, M. Yoneda, N. Fujisawa, H. Takahashi, A. Nakajima, Blockade of leukotriene B4 signaling pathway induces apoptosis and suppresses cell proliferation in colon cancer, J. Pharmacol. Sci., 103 (2007) 24-32.

[22] R. Hammamieh, M. Jett, Potential roles for inhibitors of arachidonic acid metabolism in prevention and treatment of breast cancer, Future Lipidol. 3 (2008) 265-271.

[23] M. Romano, A. Catalano, M. Nutini, E. D'Urbano, C. Crescenzi, J. Claria, R. Libner, G. Davi, A. Procopio, 5-lipoxygenase regulates malignant mesothelial cell survival: involvement of vascular endothelial growth factor, FASEB J., 15 (2001) 2326-2336.

[24] P. Yang, Z. Sun, D. Chan, C.A. Cartwright, M. Vijjeswarapu, J. Ding, X. Chen, R.A. Newman, Zyflamend® reduces LTB4 formation and prevents oral carcinogenesis in a 7, 12-dimethylbenz [α] anthracene (DMBA)-induced hamster cheek pouch model, Carcinogenesis, 29 (2008) 2182-2189.

[25] H. Asako, P. Kubes, J. Wallace, T. Gaginella, R.E. Wolf, D.N. Granger, Indomethacin-induced leukocyte adhesion in mesenteric venules: role of lipoxygenase products, Am. J. Physiol. Gastrointest. Liver Physiol., 262 (1992) 903-908.

[26] L.Y. Ma, L.P. Pang, B. Wang, M. Zhang, B. Hu, D.Q. Xue, K.P. Shao, B.L. Zhang, Y. Liu, E. Zhang, H.M. Liu, Design and synthesis of novel 1,2,3-triazole-pyrimidine hybrids as potential anticancer agents, Eur. J. Med. Chem., 86 (2014) 368-380.

[27] A.T. Mavrova, D. Wesselinova, J.A. Tsenov, L.A. Lubenov, Synthesis and antiproliferative activity of some new thieno[2,3-d] pyrimidin-4(3H)-ones containing 1,2,4-triazole and 1,3,4-thiadiazole moiety, Eur. J. Med. Chem., 86 (2014) 676-683.

[28] B. Jiang, Y. Zeng, M.-J. Li, J.-Y. Xu, Y.-N. Zhang, Q.-J. Wang, N.-Y. Sun, T. Lu, X.-M. Wu, Design, Synthesis, and Biological Evaluation of 1, 5-Diaryl−1, 2, 4−triazole Derivatives as Selective Cyclooxygenase−2 Inhibitors, Arch. Pharm., 343 (2010) 500-508.

[29] B. Jiang, X.-J. Huang, H.-Q. Yao, J.-Y. Jiang, X.-M. Wu, S.-Y. Jiang, Q.-J. Wang, T. Lu, J.-Y. Xu, Discovery of potential anti-inflammatory drugs: diaryl-1, 2, 4-triazoles bearing N-hydroxyurea moiety as dual inhibitors of cyclooxygenase-2 and 5-lipoxygenase, Org. Biomol. Chem., 12 (2014) 2114-2127.

[30] Y. Koshihara, T. Neichi, S. Murota, A. Lao, Y. Fujimoto, T. Tatsuno, Caffeic acid is a selective inhibitor for leukotriene biosynthesis, Biochim. Biophys. Acta, 792 (1984) 92-97.

[31] D. De Lucia, O.M. Lucio, B. Musio, A. Bender, M. Listing, S. Dennhardt, A. Koeberle, U. Garscha, R. Rizzo, S. Manfredini, O. Werz, S.V. Ley, Design, synthesis and evaluation of semi-synthetic triazole-containing caffeic acid analogues as 5-lipoxygenase inhibitors, Eur. J. Med. Chem., 101 (2015) 573-583.

[32] C.A. Gomes, T.G. da Cruz, J.L. Andrade, N. Milhazes, F. Borges, M.P.M. Marques, Anticancer activity of phenolic acids of natural or synthetic origin: A structure-activity study, J. Med. Chem., 46 (2003) 5395-5401.

[33] S. Fiuza, C. Gomes, L. Teixeira, M.G. Da Cruz, M. Cordeiro, N. Milhazes, F. Borges, M. Marques, Phenolic acid derivatives with potential anticancer properties—a structure–activity relationship study. Part 1: Methyl, propyl and octyl esters of caffeic and gallic acids, Biorg. Med. Chem., 12 (2004) 3581-3589.

[34] Y.-Y. Lee, C.-L. Kao, P.-H. Tsai, T.-H. Tsai, S.-H. Chiou, W.-F. Wu, H.-H. Ku, T.-T. Wong, Caffeic acid phenethyl ester preferentially enhanced radiosensitizing and increased oxidative stress in medulloblastoma cell line, Childs Nerv. Syst., 24 (2008) 987-994.

[35] J. Tai, S. Cheung, M. Wu, D. Hasman, Antiproliferation effect of Rosemary (Rosmarinus officinalis) on human ovarian cancer cells in vitro, Phytomedicine, 19 (2012) 436-443.

[36] R. Sharmila, S. Manoharan, Anti-tumor activity of rosmarinic acid in 7, 12-dimethylbenz (a) anthracene (DMBA) induced skin carcinogenesis in Swiss albino mice, Indian J. Exp. Biol., 50 (2012) 187.

[37] D. Picot, P.J. Loll, R.M. Garavito, The X-ray crystal structure of the membrane protein prostaglandin H2 synthase-1, Nature, 367 (1994) 243-249.

[38] C. Luong, A. Miller, J. Barnett, J. Chow, C. Ramesha, M.F. Browner, Flexibility of the NSAID binding site in the structure of human cyclooxygenase-2, Nat. Struct. Mol. Biol., 3 (1996) 927-933.

[39] R.G. Kurumbail, A.M. Stevens, J.K. Gierse, J.J. McDonald, R.A. Stegeman, J.Y. Pak, D. Gildehaus, J.M. Miyashiro, T.D. Penning, K. Seibert, Structural basis for selective inhibition of cyclooxygenase-2 by anti-inflammatory agents, Nature, 384 (1996) 644-648.

[40] J. Vane, Y. Bakhle, R. Botting, Cyclooxygenases 1 and 2, Annu. Rev. Pharmacool. Toxicol., 38 (1998) 97-120.

[41] N. Pommery, T. Taverne, A. Telliez, L. Goossens, C. Charlier, J. Pommery, J.-F. Goossens, R. Houssin, F. Durant, J.-P. Hénichart, New COX-2/5-LOX inhibitors: apoptosis-inducing agents potentially useful in prostate cancer chemotherapy, J. Med. Chem., 47 (2004) 6195-6206.

[42] N.C. Gilbert, S.G. Bartlett, M.T. Waight, D.B. Neau, W.E. Boeglin, A.R. Brash, M.E. Newcomer,

The structure of human 5-lipoxygenase, Science, 331 (2011) 217-219.

[43] Y. Wu, C. He, Y. Gao, S. He, Y. Liu, L. Lai, Dynamic modeling of human 5-lipoxygenase–inhibitor interactions helps to discover novel inhibitors, J. Med. Chem., 55 (2012) 2597-2605.

[44] J. Bieniek, C. Childress, M.D. Swatski, W. Yang, COX−2 inhibitors arrest prostate cancer cell cycle progression by down−regulation of kinetochore/centromere proteins, Prostate, 74 (2014) 999-1011.

[45] H. Li, F. Zhu, L.A. Boardman, L. Wang, N. Oi, K. Liu, X. Li, Y. Fu, P.J. Limburg, A.M. Bode, Aspirin prevents colorectal cancer by normalizing EGFR expression, EBioMedicine, 2 (2015) 447-455.

[46] Y.-B. Li, Z.-Q. Wang, X. Yan, M.-W. Chen, J.-L. Bao, G.-S. Wu, Z.-M. Ge, D.-M. Zhou, Y.-T. Wang, R.-T. Li, IC-4, a new irreversible EGFR inhibitor, exhibits prominent anti-tumor and anti-angiogenesis activities, Cancer Lett., 340 (2013) 88-96.

[47] S. Lin, Y. Yan, Y. Liu, C.Z. Gao, D. Shan, Y. Li, B. Han, Sensitisation of human lung adenocarcinoma A549 cells to radiotherapy by Nimotuzumab is associated with enhanced apoptosis and cell cycle arrest in the G2/M phase, Cell Biol. Int., 39 (2015) 146-151.

[48] O. Trott, A.J. Olson, Software News and Update AutoDock Vina: Improving the Speed and Accuracy of Docking with a New Scoring Function, Efficient Optimization, and Multithreading, J. Comput. Chem., 31 (2010) 455-461.

[49] B. Shi, R. Cao, W. Fan, L. Guo, Q. Ma, X. Chen, G. Zhang, L. Qiu, H. Song, Design, synthesis and in vitro and in vivo antitumor activities of novel bivalent β-carbolines, Eur. J. Med. Chem., 60 (2013) 10-22.

Highlights (for review)

- Novel COX-2/5-LOX dual inhibitors were designed via pharmacophore hybrid approach.
- Most compounds showed COX-2/5-LOX inhibitory and anti-proliferative activities.
- The compound **15c** was found to induce apoptosis and G2/M phase cell cycle arrest.
- The most potent compound **22b** significantly inhibited tumor growth *in vivo*.
- The docking studies revealed possible binding mode of these compounds.